

Identifying the Stream Depletion Paradox by Monitoring a Stream's Response to Aquifer Pumping
from Neighboring Wells

A Project
presented to
the Faculty of California Polytechnic State University,
San Luis Obispo

In Partial Fulfillment
of the Requirements for the Degree
Master of Science in Environmental Sciences and Management

by
James Klueber
September 2023

© 2023

James Klueber

ALL RIGHTS RESERVED
COMMITTEE MEMBERSHIP

TITLE: IDENTIFYING THE STREAM DEPLETION
PARADOX BY MONITORING A STREAM'S
RESPONSE TO AQUIFER PUMPING FROM
NEIGHBORING WELLS

AUTHOR: James Klueber

DATE SUBMITTED: September 2023

COMMITTEE CHAIR: Bwalya Malama, Ph.D.
Professor of Groundwater and Soil Biophysics

ABSTRACT

IDENTIFYING THE STREAM DEPLETION PARADOX BY MONITORING A STREAM'S RESPONSE TO AQUIFER PUMPING FROM NEIGHBORING WELLS

James Klueber

Current groundwater models utilize a constant head (Dirichlet) boundary condition which assumes stream stage is fixed and does not experience any drawdown in the event of pumping from an interconnected aquifer despite the presence of stream depletion. Therefore, constant head boundary implies that streams and lakes in a groundwater model behave as an infinite supply of water when aquifer pumping occurs. This study aimed to determine if a stream located in the California Central Coast experiences drawdown and depletion when pumping occurs within an aquifer-stream system. This was achieved by measuring stream stage, aquifer water levels, stream discharge, and the hydraulic conductivity of the subject streambed. Passively collected stream stage and aquifer water level data, actively collected stream discharge data, and in-situ streambed hydraulic conductivity measurements were taken from August 2022 to August 2023 and analyzed using time series analyses and hydraulic conductivity calculation methods. This study confirmed that stream depletion occurred during aquifer pumping and, at low discharge rates, stream stage exhibits observable drawdown in response to aquifer pumping which contradicts the constant head boundary assumption and confirms the existence of the stream depletion paradox in the subject aquifer-stream system. The streambed hydraulic conductivity was found to be relatively high and contained highly conductive gravels and coarse sands implying that the streambed has relatively high storage capacity in the subject stream. This research, subsequent data collection, and improvements to groundwater modeling will allow water managers and planners to sustainably manage local water resources which will be relied upon for generations to come.

Keywords: stream depletion; stream discharge; drawdown; streambed hydraulic conductivity; aquifer; SGMA

ACKNOWLEDGMENTS

I first would like to thank my advisor, Dr. Bwalya Malama, for his consistent support throughout this research project. I feel very fortunate to have been guided and mentored by one of the leading academics in groundwater hydrology. It would not have been possible to complete this project without his guidance and patience in my endeavor to learn by doing. I would also like to thank Dr. Christopher Surfleet and the entire CAFES faculty and staff for their guidance throughout my Cal Poly experience. A special thank you to Sara Sternberg, Daniel Seiler, and my MS ESM peers for their guidance, assistance, and support throughout the program. I would also like to thank my girlfriend, Gabriella Cuevas, for supporting my dream and encouraging me every step of the way in the process of earning my graduate degree. Lastly, I would like to thank my parents, Darrell Klueber, and Ann Parker, who have given me unwavering support and have been my source of inspiration throughout my life. Their passion for environmental stewardship is instilled in me and has ultimately led down this path to obtain a master's degree in environmental sciences and management.

TABLE OF CONTENTS

	Page
LIST OF TABLES.....	viii
LIST OF FIGURES	ix
<u>CHAPTER 1: INTRODUCTION</u>	<u>1</u>
<u>CHAPTER 2: LITERATURE REVIEW</u>	<u>6</u>
2.1 IMPACTS OF AQUIFER PUMPING ON SURFACE WATER RESOURCES.....	6
2.2 GROUNDWATER AND SURFACE WATER MODELING	7
2.2.1. ANALYTICAL MODELS.....	8
2.2.2. NUMERICAL MODELS	10
2.2.3. RECENT INNOVATIONS IN GROUNDWATER MODELING	10
2.3 STREAM STAGE MONITORING.....	11
2.4 STREAM DISCHARGE MEASURING	11
2.5 AQUIFER WATER LEVEL MONITORING	12
2.6 STREAMBED HYDRAULIC CONDUCTIVITY	13
<u>CHAPTER 3: METHODOLOGY</u>	<u>15</u>
3.1 STUDY SITE DESCRIPTION.....	15
3.2 DATA COLLECTION.....	18
3.2.1. PASSIVE DATA COLLECTION	19
3.2.2. STREAM DISCHARGE MEASUREMENTS.....	21
3.2.3. STREAMBED CONDUCTIVITY MEASUREMENTS.....	24
3.3 STREAM STAGE AND AQUIFER WATER LEVEL DATA ANALYSIS	29
3.4 STREAM DISCHARGE DATA ANALYSIS.....	31
3.5 STREAMBED CONDUCTIVITY DATA ANALYSIS	32
3.6 LIMITATIONS.....	34
<u>CHAPTER 4: RESULTS</u>	<u>37</u>
4.1 STREAM STAGE RESPONSE TO AQUIFER PUMPING.....	37
4.1.1 TIME SERIES ANALYSIS OF STREAM STAGE AND AQUIFER WATER LEVELS AT THE LEMON ORCHARD SITE	37
4.1.2 SPECTRAL ANALYSIS OF STREAM STAGE AND AQUIFER WATER LEVELS AT THE LEMON ORCHARD SITE	42
4.1.3 TIME SERIES ANALYSIS OF STREAM STAGE AND AQUIFER WATER LEVELS AT THE FIELD 25 SITE.....	51

4.1.4 SPECTRAL ANALYSIS OF STREAM STAGE AND AQUIFER WATER LEVELS AT THE FIELD 25 SITE.....	52
4.2 STREAM DISCHARGE RESPONSE TO AQUIFER PUMPING	56
4.3 STREAMBED HYDRAULIC CONDUCTIVITY	58
4.3.1 LEMON ORCHARD REACH PNEUMATIC SLUG TEST RESULTS.....	59
4.3.2 FIELD 25 REACH PNEUMATIC SLUG TEST RESULTS	62
<u>CHAPTER 5: DISCUSSION.....</u>	<u>66</u>
5.1. STREAM STAGE RESPONSE TO AQUIFER PUMPING.....	66
5.2. STREAM DISCHARGE RESPONSE TO AQUIFER PUMPING	68
5.3. STREAMBED HYDRAULIC CONDUCTIVITY	69
5.4. FUTURE CONSIDERATIONS	71
<u>CHAPTER 6: CONCLUSION.....</u>	<u>73</u>
<u>REFERENCES</u>	<u>75</u>

LIST OF TABLES

Table	Page
Table 3.1 AQTESOLV Input Format	34
Table 4.1 Maximum observable drawdown duration and quantity in the aquifer at ABD-MW during 2022 Dry Season pumping events.	40
Table 4.2 Maximum observable drawdown duration and quantity in Stenner Creek at LO-P1 during 2022 Dry Season pumping events.	40
Table 4.3 Maximum observable drawdown duration and quantity in aquifer at ABD-MW during 2023 Dry Season pumping events.	42
Table 4.4 Stenner Creek discharge rates recorded at the Field 25 site.....	58
Table 4.5 Typical hydraulic conductivity values of water bearing materials.....	58
Table 4.6 Pneumatic slug test results at the Lemon Orchard reach.	62
Table 4.7 Pneumatic slug test results at the Field 25 reach.....	65

LIST OF FIGURES

Figure	Page
Figure 3.1 Map of the San Luis Obispo Creek Watershed and project location.	17
Figure 3.2 Overview map of Field 25 and Lemon Orchard pumping wells, monitoring wells, and in-stream piezometers.	18
Figure 3.3 Stream stage monitoring equipment and in-stream measuring sites.	20
Figure 3.4 Stream discharge equipment and usage at the Lemon Orchard site.	22
Figure 3.5 Stream discharge measuring locations at the Lemon Orchard and Field 25 sites.	23
Figure 3.6 Streambed pneumatic slug test equipment and researcher using equipment.	26
Figure 3.7 Map of the Lemon Orchard study site.	28
Figure 3.8 Map of the Field 25 study site.	29
Figure 3.9 Example of streambed slug test raw data in a scatter plot.	33
Figure 3.10 Example of extracted streambed slug test displacement scatter plots to be used in AQTESOLV.	33
Figure 4.1 Stream stage and aquifer water levels from Aug. 2022 to Aug. 2023 at Lemon Orchard site.	38
Figure 4.2 Stenner Creek stream stage and aquifer water level at Lemon Orchard site during 2022 Dry Season with pumping events identified.	39
Figure 4.3 Stenner Creek stream stage and aquifer water level at Lemon Orchard site during 2023 Dry Season with pumping events identified.	41
Figure 4.4 Spectral analysis of LO-P1 for 2022 Dry Season. Respectively, a) raw data, b) raw data detrended, c) reconstructed data with cubic polynomial fit, d) reconstructed and detrended data, e) residuals represented as difference between reconstructed and detrended data, and f) power spectra with frequencies with major and minor signals identified.	45
Figure 4.5 Spectral analysis of ABD-MW for 2022 Dry Season. Respectively, a) raw data, b) raw data detrended, c) reconstructed data with cubic polynomial fit, d) reconstructed and detrended data, e) residuals represented as difference between reconstructed and detrended data, and f) power spectra with frequencies with major and minor signals identified.	46
Figure 4.6 Spectral analysis of LO-P1 for 2023 Dry Season from April 26 to June 2. Respectively, a) raw data, b) raw data detrended, c) reconstructed data with cubic polynomial fit, d) reconstructed and detrended data, e) residuals represented as difference between reconstructed and detrended data, and f) power spectra with frequencies with major and minor signals identified.	47
Figure 4.7 Spectral analysis of ABD-MW for 2023 Dry Season from April 26 to June 2. Respectively, a) raw data, b) raw data detrended, c) reconstructed data with cubic polynomial fit, d) reconstructed and detrended data, e) residuals represented as difference between reconstructed and detrended data, and f) power spectra with frequencies with major and minor signals identified.	48
Figure 4.8 Spectral analysis of LO-P1 for 2023 Dry Season from June 9 to August 14. Respectively, a) raw data, b) raw data detrended, c) reconstructed data with cubic polynomial fit, d) reconstructed and detrended data, e) residuals represented as difference between reconstructed and detrended data, and f) power spectra with frequencies with major and minor signals identified.	49
Figure 4.9 Spectral analysis of ABD-MW for 2023 Dry Season from June 9 to August 14. Respectively, a) raw data, b) raw data detrended, c) reconstructed data with cubic polynomial fit, d) reconstructed and detrended data, e) residuals represented as difference between	

reconstructed and detrended data, and f) power spectra with frequencies with major and minor signals identified.	50
Figure 4.10 Dry Stenner Creek at F25-P1 stream stage monitoring location on 8/11/2023.	51
Figure 4.11 Stenner Creek stream stage and aquifer water level at Field 25 site during 2023 Dry Season.	52
Figure 4.12 Spectral analysis of F25-P1 for 2023 Dry Season. Respectively, a) raw data, b) raw data detrended, c) reconstructed data with cubic polynomial fit, d) reconstructed and detrended data, e) residuals represented as difference between reconstructed and detrended data, and f) power spectra with frequencies with major and minor signals identified.....	54
Figure 4.13 Spectral analysis of F25-PW for 2023 Dry Season. Respectively, a) raw data, b) raw data detrended, c) reconstructed data with cubic polynomial fit, d) reconstructed and detrended data, e) residuals represented as difference between reconstructed and detrended data, and f) power spectra with frequencies with major and minor signals identified.....	55
Figure 4.14 Stream discharge in Stenner Creek and aquifer water level in ABD-MW at Lemon Orchard site during 2023 Dry Season.	57
Figure 4.15 Stenner Creek slug test location images at the Lemon Orchard reach.	61
Figure 4.16 Stenner Creek slug test location images at the Field 25 reach.	64

CHAPTER 1: INTRODUCTION

Water is needed to support all aspects of human societies, economies, and our surrounding environment, yet it is a scarce resource in the western United States. The primary sources of water accessible to humans are surface water (e.g., streams, rivers, and creeks), and subsurface groundwater all of which are connected through the hydrologic cycle (Winter et al., 1998). Prolonged droughts have an immediate impact on surface water quantities by reducing precipitation rates over a given drought period (DWR, 2023). Over the past two decades, California and much of the western United States have experienced prolonged drought conditions leading to depletion of surface water resources (“West | U.S. Drought Monitor” 2023). The absence of historic surface water quantities and subsequent curtailment of surface water diversions has motivated water resource management agencies to utilize alternative water sources, such as groundwater, to satisfy water demands (Hansen, 2017).

Groundwater is considered one of the most valuable water resources because it does not experience evaporation losses perpetuated by drier climates and can be used as a “water bank” (Miro & Famiglietti, 2019). The term “water banking” is the aquifer management practice in which aquifers are recharged naturally (e.g., percolation from precipitation) or artificially (e.g., direct injection or surface spreading) during high surface water flows to replenish and expand groundwater reserves. In times of drought, the stored groundwater is extracted and used to satisfy water demands (Kenny et al., 2009). Water banking is especially important in California considering drought conditions have plagued the entire state and, by implementing this practice, water users improve their water supply resiliency to short term drought impacts (WEF, 2020). In response to prolonged drought conditions in California, water managers have turned to local groundwater resources as the primary water source, which has led to a mismanagement and overdraft of aquifers throughout the State (Thomas, 2019). In response to this mismanagement of aquifers and to protect these valuable “water banks” from being over drafted, the California State Legislature passed the Sustainable Groundwater Management Act (SGMA) in 2014, which identifies critically over drafted basins and requires local jurisdictions to develop and adopt

Groundwater Sustainability Plans (GSPs) in order to ensure California groundwater basins are managed sustainably and protected from overuse (Miro & Famiglietti, 2019). SGMA has identified six factors indicating the mismanagement of an aquifer: chronic groundwater elevation decline, surface water depletion (between interconnected surface and subsurface water resources), degradation in water quality, sea water intrusion, subsidence, and loss of groundwater storage (DWR, 2016).

From January to April 2023, California experienced record high precipitation, which replenished much of California's snowpack, surface water reservoirs, and rivers (DWR 2023b). This excess surface water has resulted in higher surface water allocations (DWR 2023a) and thus higher water banking rates as water managers prepare for the next extended drought period (Waterworld 2023). Although this winter has provided immediate relief to current short-term drought conditions, prolonged droughts will continue to motivate water managers to sustainably manage groundwater systems to protect their limited water supplies.

Water management agencies with jurisdiction over aquifers rely on hydrologic and hydraulic models (collectively referred to as "groundwater models") to forecast water availability under various conditions. Hydraulic models depict the flow of fluids within a given medium whereas hydrologic models depict the transition of precipitation into runoff or surface water discharge (USGS, 2023). These models are often used in unison by water managers for forecasting, sensitivity analyses, and other critical analyses to ensure surface and groundwater resources are managed appropriately (USGS 2023). Therefore, accurate groundwater modeling is essential to effective water management given the scarcity of water resources and subsequent legislation, such as SGMA. As stated by Miro and Famiglietti (2019), being able to predict the impacts of groundwater pumping or surface water diversions on the water supply source itself and surrounding environment is imperative to water supply forecasting considering the interconnection of these water resources throughout the State. From a legal perspective,

pumping from an interconnected aquifer-surface water system based on a flawed model could result in the drying of the surface water resource, which would infringe on downstream surface water rights (Miro & Famiglietti, 2019). From an environmental perspective, the drying of the stream due to over pumping could lead to the degradation of riparian ecosystems that rely on surface water for survival. The mismanagement of water resources due to inaccurate groundwater modeling would jeopardize our limited water resources causing a multitude of negative environmental, economic, and societal impacts (Miro & Famiglietti, 2019).

A key component to hydraulic modeling is determining the hydraulic conductivity (K), the ability of the fluid to pass through the pores and fractured rocks (Saravanan et al., 2019, p. 10), and hydraulic connectivity, the ability for water to flow between two water bodies (Brodie et al., 2007), within a hydrologic system and how hydraulic connectivity and conductivity influence water levels at various points throughout the system when pumping occurs. Theis (1935) studied the response of groundwater levels during pumping from a confined aquifer which developed a solution for predicting drawdown observed within an interconnected aquifer system. However, for the Theis solution to be valid, many simplifying assumptions are required such as aquifer isotropy and homogeneity, an infinite radial extent of the aquifer and other assumptions. In a later study by Theis (1941), he determined that groundwater pumping from connected aquifers can affect stream discharge while the stream is assumed to be a fixed stage, or a constant head (Dirichlet) boundary condition. This has led to several studies being developed that have sought to improve the accuracy of the Theis solution. However, these studies continued upon the assumption that a change in stream discharge due to aquifer pumping will have no impact on stream stage and only proposed theoretical solutions without field data to support their findings (Baalousha, 2012; Hunt, 2014; Wang et al., 2016; Ward & Callander, 2010; Zlotnik et al., 1999).

Since the introduction of the Theis solution and subsequent refinements to groundwater models, all subsequent solutions to the groundwater flow problem impose either a constant head

(Dirichlet) or general (Robin) condition for the groundwater flow problem to be solvable (Malama et al., 2022). Both conditions assume that stream stage (or head) is constant and does not experience any drawdown (reduction in stage) in the event of pumping from an interconnected aquifer. This implies that streams and lakes in such a groundwater model act as an infinite supply of water. This case of stream depletion without stream drawdown is referred to as the stream depletion paradox in Malama et al. (2022).

This paradox within existing groundwater modeling methods presents a research gap. To better model the effects of groundwater pumping on stream discharge and stage, there needs to be refinements to the existing groundwater models that takes into consideration the geologic properties of the stream namely the streambed hydraulic conductivity and the finite nature of streambed storage. By collecting stream discharge, stream stage, and aquifer water level data under various pumping scenarios coupled with data detailing the hydraulic conductivity of the streambed, the following hypotheses were developed:

Hypothesis 1 (H1): Pumping from an aquifer will reduce stream stage in an aquifer-stream system.

Hypothesis 2 (H2): Pumping from an aquifer will cause stream depletion in in an aquifer-stream system.

Hypothesis 3 (H3): Higher degrees of change in stream stage and discharge will occur in segments of the stream that are more hydraulically conductive and thus higher storage capacity.

To test these hypotheses, stream stage, discharge, and aquifer water level data recorded near groundwater pumping wells in the vicinity of Stenner Creek on the California Polytechnic University, San Luis Obispo (Cal Poly) campus were collected and analyzed. Additionally, the streambed hydraulic conductivity was measured within two reaches of Stenner Creek. Through

data collection and analysis, the stream stage and discharge responses to aquifer pumping were compared. Malama et al. (2022) developed a model that is designed to improve the accuracy of groundwater models; however, the model needs to be validated with field data. This project seeks to expand upon the field research portion of this study and to determine the hydraulic conductivity of the streambed and interconnectedness of the stream to the underlying aquifer. The methods, results and discussion below will provide future researchers a process to identify, collect, and refine inputs to groundwater models and water budgeting process by accounting for the effects of aquifer pumping on neighboring streams. This research and subsequent improvements to groundwater modeling will allow water managers and planners to sustainably manage local water systems.

CHAPTER 2: LITERATURE REVIEW

2.1 Impacts of Aquifer Pumping on Surface Water Resources

The distribution and availability of freshwater is a major concern to water resource planners (Barlow et al., 2003; Berbel & Esteban, 2019; Miro & Famiglietti, 2019). Considering the impacts of climate change to usable water supplies (Berbel & Esteban, 2019) and that the amount of freshwater accessible to humans is only 0.3% of the amount of water on earth (Mullen 2022), accurately modeling freshwater dynamics is critical to effective water management (USGS, 2023). Freshwater is vital to every aspect of our social, economic, and environmental systems (Kenny et al., 2009). In particular, aquifers are essential for water resource management in California considering aquifers are able to be recharged, naturally or artificially, during times of excess surface water and extracted from in times of drought (Berbel & Esteban, 2019; de Wrachien & Fasso, 2002; Miro & Famiglietti, 2019). This conjunctive use of groundwater and surface water under prolonged drought conditions has resulted in overuse of aquifers and a slew of negative consequences impacting all aspects of California (Miro & Famiglietti, 2019). Groundwater overuse has shown to affect stream flow, water quality, water quantity, groundwater storage, and other issues (Thomas 2019; Miro and Famiglietti 2019; DWR 2016). The overuse of aquifers has resulted in many basins being over drafted basin in California (Miro & Famiglietti, 2019; Thomas, 2019) and the subsequent passing of SGMA in 2014 to address overdraft issues (State of California, 2014).

Climate change coupled with mismanagement of water resources will reduce the quantity of freshwater supplies available for human uses and riparian habitats, which will have negative consequences on our economies, societies, and the environment (Miro & Famiglietti, 2019). These negative consequences from aquifer overdraft are realized today such as reduced availability of groundwater in the Central Valley (Miro & Famiglietti, 2019), salt water contamination of coastal aquifers (DWR 2016), and habitat degradation (Miro & Famiglietti, 2019). With the expected increase in drought frequency, drought duration, and subsequent water resource depletion, it is expected the use of groundwater resources will increase (Miro &

Famiglietti, 2019). The threat of groundwater overuse is being addressed through the implementation of SGMA and the sustainable management of our groundwater and surface water resources (Miro & Famiglietti, 2019). A key component to sustainable water management is refinement of the hydrologic and hydraulic modeling methods used to predict the impacts of groundwater pumping on stream flows (Foglia et al., 2018).

2.2 Groundwater and Surface Water Modeling

Research has shown that streams and aquifers are interconnected and should be treated as a single source of water (Winter et al., 1998). When surface water and aquifers are treated as separate sources, a variety of issues ensue (Winter et al., 1998). These issues include freshwater supply depletion, water quality degradation, and degradation of aquatic environments (Winter et al. 1998; DWR 2016). To address and manage these issues caused by freshwater mismanagement, it is important to acknowledge and account for the interactions of surface water and aquifer sources when developing groundwater and hydrologic models (Foglia et al., 2018; Winter et al., 1998).

Theis (1941) developed a transient model to depict the temporal relationship between hydraulically connected aquifers and streams. Specifically, this study predicted the effects of a pumping well on a nearby, hydraulically connected, stream (Theis, 1941). This study developed a solution that is still utilized by hydrologists and water resource planners today. Theis's solution is designed to predict the amount of drawdown observed at a given point within an aquifer system as a result of groundwater pumping (Theis, 1935). However, the solution is only valid under simplified assumptions such as aquifer isotropy and homogeneity, the infinite radial extent of the subject aquifer, and other simplifying assumptions (Theis, 1941). There have been many adaptations, refinements, and tangential models developed, which built upon the Theis (1941) solution and are designed to provide a more accurate representation of an aquifer system. In

relation to this study, the types of models that have been developed in the literature can be categorized into analytical models and numerical models as discussed in more detail below.

2.2.1. Analytical Models

Analytical models are mathematical models that have a closed form solution of the groundwater flow equation (Baudic et al., 2021). In the context of aquifer-stream connectivity modeling, analytical models are developed to provide blanket solutions to theoretical scenarios (Lough & Hunt, 2006). Despite the generalization of Theis's solution, the result of Theis's research determined that pumping near a stream that has measurable discharge is likely to diminish the stream discharge rate. Conversely, diverting water from a stream thereby reducing the seepage into the aquifer would reduce the amount of groundwater available (Theis, 1941).

Glover and Balmer (1954) extended upon the Theis method by developing a closed-form function of the Theis model providing exact solutions to the groundwater flow problem. Jenkins (1968) performed tabulations of the Glover Balmer formula which computed the rate of stream depletion anytime during the pumping period, the volume induced from the stream during anytime during the pumping cycle, and the rate and volume of stream depletion of any selected intermittent pumping (Jenkins, 1968). Other iterations and refinements of analytical models were developed to consider various hydraulic conditions. Some key hydraulics conditions modeled include; semipervious streambeds with a general boundary condition (Robin Boundary) (Hantush, 1965), confined aquifers bounded by intersecting streams (Chan, 1976), partially penetrating streams (Zlotnik et al., 1999), and an unconfined aquifer condition (Hunt, 2003). These studies have perpetuated the development of analytical models which utilize the constant head boundary condition in the presence of a stream.

The study performed by Zlotnik et al. (1999) is significant to this research because it extended the analytical stream depletion model to the case of partially penetrating streams. This model incorporates the effects of finite stream width, shallow stream penetration, and a low permeability streambed. The key assumption of this model is the Dupuit assumptions of steady state flow across the streambed (Zlotnik et al., 1999). This adaptation of the aquifer-stream connectivity model is important to this research paper because the partially penetrating model can be utilized for a variety of analyses when conducting aquifer-stream connectivity as exemplified in the work performed by (Hunt, 2009).

Key studies to determining the methodology of this study include Hunt (2003 & 2009) which performed stream depletion models where the aquifer is unconfined. (Hunt, 2003) developed a solution for flow to a well beside a stream in a semiconfined aquifer system through analyzing field data obtained from a previous study performed by Weir (1999). The Hunt (2003) study compared an analytical solution which assumes the pumped aquifer is bounded on top by a semipermeable aquitard containing a shallow water table, and the stream partially penetrates the aquitard, with the field data collected by Weir. This comparison resulted in the new solution developed by Hunt, which provides improved description of the experimental data (Hunt, 2009). In 2009, Hunt developed a semi-analytical stream depletion solution for pumping a well beside a stream in a two-layer leaky aquifer system. Hunt concluded that a stream depletion solution for a single aquifer solution closely approximates the two-aquifer solution when the single aquifer transmissivity is replaced with the sum of transmissivities of the two systems (Hunt, 2009).

The evolution of analytical models discussed above provides an overview of the development of groundwater water modeling. This study is designed to address the limitation of the above stated analytical models that utilize a constant head, or fixed stream stage, boundary and therefore assume streams are an indefinite source of water regardless of pumping rates. These analytical

methods and models are used in conjunction with one another to perform numerical modeling as discussed below.

2.2.2. Numerical Models

Numerical models differ from analytical models in that numerical models are a combination of large number of mathematical equations that depend on computers to find an approximate solution to the underlying physical problem (Chanson, 2004). In the context of groundwater-surface water modeling, three numerical models were identified namely MODFLOW (Harbaugh, 2005), HydroGeoSphere (Brunner & Simmons, 2011), and MIKE SHE (Jaber & Shukla, 2012). These models treat stream boundary conditions and the source/drainage terms in a manner like the analytical models. These models also allow for researchers to characterize the spatially variable stream stage through the usage of empirical hydrographs or formulas. These numerical models are computationally difficult and time intensive as they require an iterative method for every step and are nonlinear.

2.2.3. Recent Innovations in Groundwater Modeling

Groundwater modeling which accounts for streamflow depletion resulting from aquifer pumping is a rapidly expanding topic of interest amongst researchers. Zipper et al. (2022) performed a practical review of past and emerging methods of quantifying streamflow depletion under groundwater pumping. In particular, this study reviews the existing analytical, and numerical models designed to estimate streamflow depletion. Huang et al. (2020), presents new models designed to predict groundwater flow in an aquifer-stream system and the joint effect of streambed width and storage on the stream depletion rate. Li et al. (2022) developed an analytical depletion function (ADF) model designed to address the shortcomings of analytical and numerical models. ADFs can be used during the preliminary screening process of determining streamflow under a variety of streamflow and aquifer pumping scenarios. These recent

innovations in conjunctive modeling of surface water and groundwater resources are imperative to sustainable management of our environmental systems.

2.3 Stream Stage Monitoring

Stream stage monitoring is a crucial element to this study to determine the stream stage drawdown in response to aquifer pumping. Most methods for stream stage monitoring utilized by researchers based in the United States are provided by the United States Geological Survey (USGS). Specifically, the USGS provides an overview of all relevant methods used to measure stream stage which includes staff gage, float type gage, and other methods (Rantz, 1982). The pressure transducer methods outlined by USGS in Freeman et al. (2004) are more applicable to this study since this study passively monitored stream stage through methods previously used by Malama et al. (2021). More information regarding the stream stage monitoring methods is discussed below.

2.4 Stream Discharge Measuring

Stream discharge data must be recorded to effectively model stream stage depletion due to aquifer pumping. This data must be collected under non-pumping and pumping conditions to characterize the stream flows (Dobriyal et al., 2017). Dobriyal et al. (2017) reviewed a variety of methods to measure stream discharge in the context of sustainable water resource management. Dobriyal et al. (2017) reviewed available methods for modeling streamflow based on their applicability across different terrains and size of streams, operational ease, time effectiveness, accuracy, environmental impact of the methods. In hilly terrains having smaller streams, the timed volume method is preferred whereas in flat terrains with smaller streams, the float method is best suited due to the operational ease and cost effectiveness. Lapidés et al. (2022) performed a demonstrative analysis on Wisconsin streams, which determined that both the magnitude and variability of streamflow and stream temperatures are likely to be impacted by groundwater withdrawal. This research is similar to this study; however, Lapidés et al. (2022) research only

accounts for stream flow, or discharge, and does not account for stream stage and streambed hydraulic conductivity within their modeling approach and analysis. This research will utilize the volume-area method (Turnipseed & Sauer, 2010) to measure the stream discharge rates as discussed further in the Methods chapter.

2.5 Aquifer Water Level Monitoring

Cherry (1990) reviewed the deficiencies and opportunities of traditional groundwater monitoring methods. Over the course of the 20th century, groundwater monitoring has evolved from a minor endeavor carried out by agricultural producers and urban water providers to a large industry. The conclusion within Cherry (1990) is that the implementation of monitoring wells provides effective information regarding the conditions of the underlying aquifer. This information is important to consider as this study utilizes monitoring wells to quantify the drawdown from the subject pumping wells. However, the observed aquifer water levels are also subject to the degree of aquifer-stream hydraulic connectivity.

Measuring aquifer water levels while monitoring stream discharge is essential for the determined methods of analyzing aquifer-stream interactions. Kalbus et al. (2006) reviewed the applicable methods for measuring groundwater-surface water interactions under various connectivity scenarios (Kalbus et al., 2006). Kalbus et. al. (2006) also provides an overview of the methods that are currently used for estimating fluxes at the groundwater-surface water interface. They considered the spatial and temporal scales, uncertainties, and limitation in estimating drawdown in a stream due to pumping. They concluded that a multi-scale approach of combining multiple measuring methods may constrain groundwater-surface water flux estimates. A component to the results of groundwater monitoring are various aquifer properties that need to be characterized as well.

2.6 Streambed Hydraulic Conductivity

The third hypothesis of this research determines the degree of hydraulic connectivity between aquifers and streams, the storage capacity of the streambed, and if there is a variation in impact of pumping on a stream that is not as hydraulically connected to the aquifer. Specifically, the variable that will be refined for this study at Stenner Creek is the hydraulic conductivity of the streambed. The origins of hydraulic conductivity and a discussion of potential methods for measuring each variable is discussed in more detail below.

Hydraulic conductivity is the ability of a fluid to pass through the pores and fractured rocks within a given matrix. This concept was first studied by Darcy (1856). The concept of hydraulic conductivity in relation to an aquifer-stream system was explored by Hantush (1965) in his study titled "Wells Near Stream with Semipervious Beds". Hantush (1965) described a procedure to determine the transmissivity, the effective distance of the stream, and the "retardation coefficient" of the channel lining. This study provides methods for determining key factors like hydraulic conductivity and transmissivity within an aquifer, however, there are a variety of methods to analyze when determining the appropriate method for hydraulic conductivity within a streambed.

The hydraulic conductivity of a streambed is a parameter that relates the head difference between the stream and aquifer water flows across the stream channel (Lackey et al., 2015). Streambed conductivity has been identified as a key parameter when testing aquifer-stream interactions (Glover & Balmer, 1954; Hantush, 1965; Hunt, 1999; Theis, 1941). However, these previous solutions assume streambed conductivity to be constant throughout the studied area which is an incorrect assumption (Lackey et al., 2015).

Considering the heterogeneity of streambeds, the streambed conductivity value is traditionally determined using numerical models (Lackey et al., 2015). These numerical models depend on

the appropriate parameterization of the hydraulic properties of the streambed, which can be difficult to obtain (Lackey et al. 2015; Baalousha 2012; Chen and Shu 2005). The study by Lackey et al., (2015) presents a methodology for performing a pump test to determine the feasible pumping well locations in proximity to the subject stream (Lackey et al., 2015).

Numerous studies have determined that streambed conductivity is a key parameter to stream depletion (Chen & Shu, 2005; Chen & Yin, 2005; Christensen, 2005; Hunt, 1999) whereas others have demonstrated an insensitivity of stream depletion to streambed conductivity (Leake et al., 2008). However, within the study presented by Lackey et al. (2015), it is demonstrated that there is a range of streambed conductivity values where stream depletion is sensitive. This was not considered within Leake et al. (2008). This study performed in-situ measurements of streambed hydraulic conductivity data throughout two reaches of Stenner Creek to determine the most prominent values of hydraulic conductivity within the streambed and assess connectivity with the aquifer system. More information on streambed conductivity testing procedure is discussed in the Methods chapter below.

CHAPTER 3: METHODOLOGY

The primary analysis components of this study include passively collected stream stage and aquifer water level data, actively collected stream discharge data under pumping and non-pumping conditions, and in-situ streambed hydraulic conductivity (K) data. All in-stream data were collected within two reaches of Stenner Creek and within two wells located in the Cal Poly agricultural fields. The following sections provide an overview of the study site, the methods used for data acquisition, and for data analysis.

3.1 Study Site Description

The study site is located adjacent to the agricultural fields of the Cal Poly campus, which is located along the central coast of California. The primary water resource for these agricultural fields is groundwater pumped from the underlying alluvial basin. This groundwater basin is designated as a medium priority basin by SGMA, which was passed by the State of California in 2014 (“SGMA Basin Prioritization Dashboard” 2023). Therefore, the results in this study are applicable to the management of this groundwater basin and its ability to achieve sustainable yield as mandated under SGMA (State of California, 2014).

The subject alluvial aquifer is confined and bounded at the top by a thin layer of saturated clayey soils and sediment of very low permeability. This layer serves as the upper confining unit and is approximately 36-ft. thick. The lower boundary of the aquifer is approximately 72-ft. deep and comprised of metavolcanic bedrock of an unknown thickness. The aquifer is measured to be approximately 36-ft. thick. The above characterizations of the aquifer were determined from well installation drilling logs in the surrounding agricultural fields provided by Cal Poly’s Agricultural Operations department (“Agricultural Operations” 2023).

The subject stream is Stenner Creek, a tributary to San Luis Obispo Creek and within the San Luis Obispo Creek watershed. The San Luis Obispo Creek discharges into the San Luis Bay

located approximately 9 miles southwest of the study site. Stenner Creek flows across the study site on top of the aquifer from northwest to southeast and cuts the entire thickness of the confining upper layer of the aquifer (Malama et al., 2022). Therefore, the stream is in direct hydraulic connection with the above-mentioned aquifer (Malama et al., 2022). The streambed is comprised of clay soils and the same sand and gravel formation as the aquifer.

The two pumping wells used for this study are in Agricultural Field 25 ("Field 25") and the Lemon Orchard located on the Cal Poly campus referred to as F25-PW and LO-PW, respectively. Field 25 is located upstream of the Lemon Orchard and is irrigated three to four days a week during dry months. The Lemon Orchard is located downstream of Field 25 and is irrigated for approximately three consecutive days every two weeks. The stream stage monitoring locations were selected based on proximity to their respective pumping well and stream characteristics as discussed below. Figure 3.1 provides a location map of the study site in relation to the regional map. Figure 3.2 provides an overview of the study site including Stenner Creek, Field 25, the Lemon Orchard, the pumping well locations and stream stage monitoring locations.

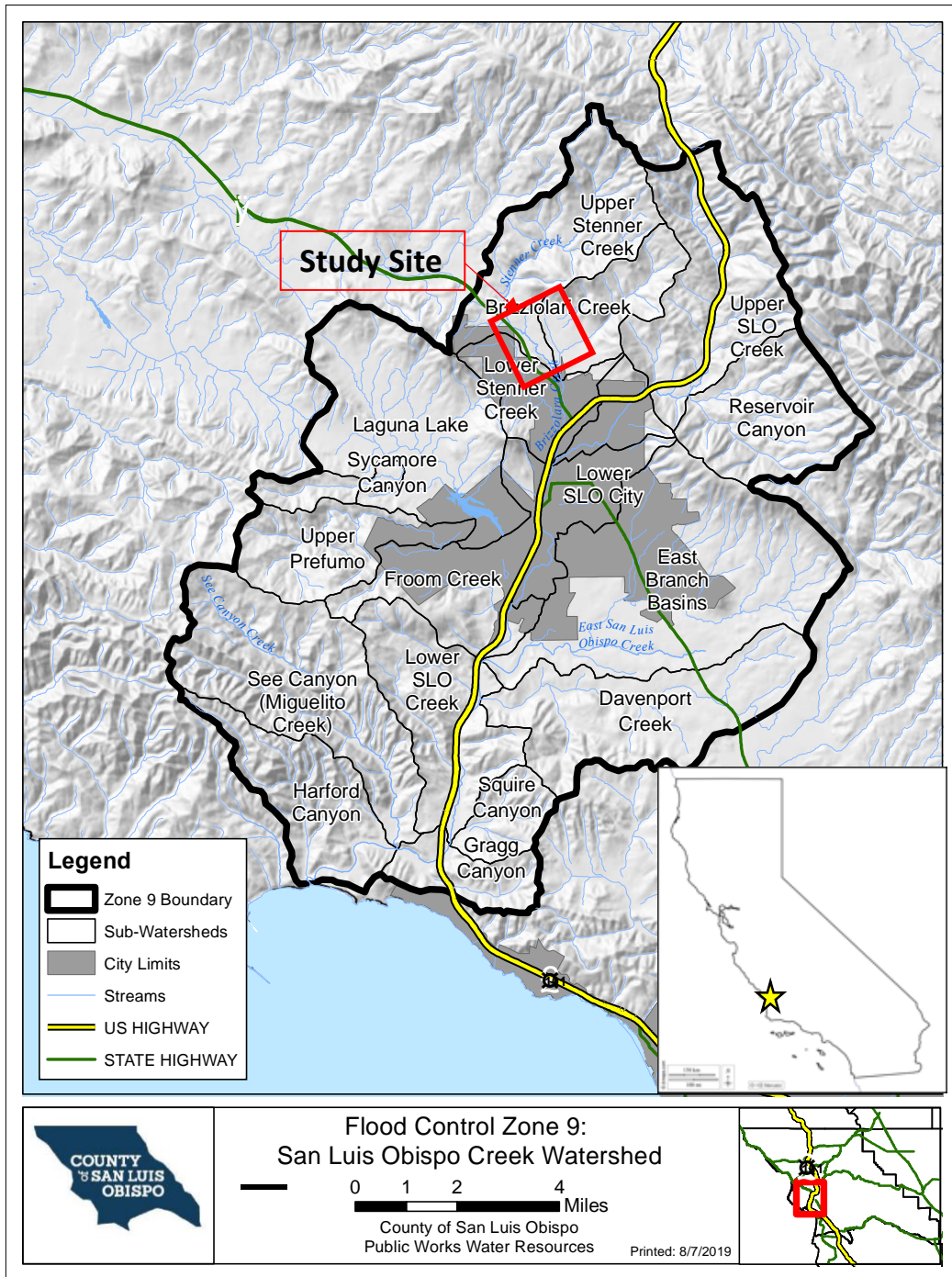


Figure 3.1 Map of the San Luis Obispo Creek Watershed and project location.¹

¹ County of San Luis Obispo Flood Control Map, San Luis Obispo Creek Watershed. 8/19/2019
<https://www.slocounty.ca.gov/Departments/Public-Works/Current-Public-Works-Projects/SLO-Watershed/Watersheds/South-County/San-Luis-Obispo-Creek.aspx>

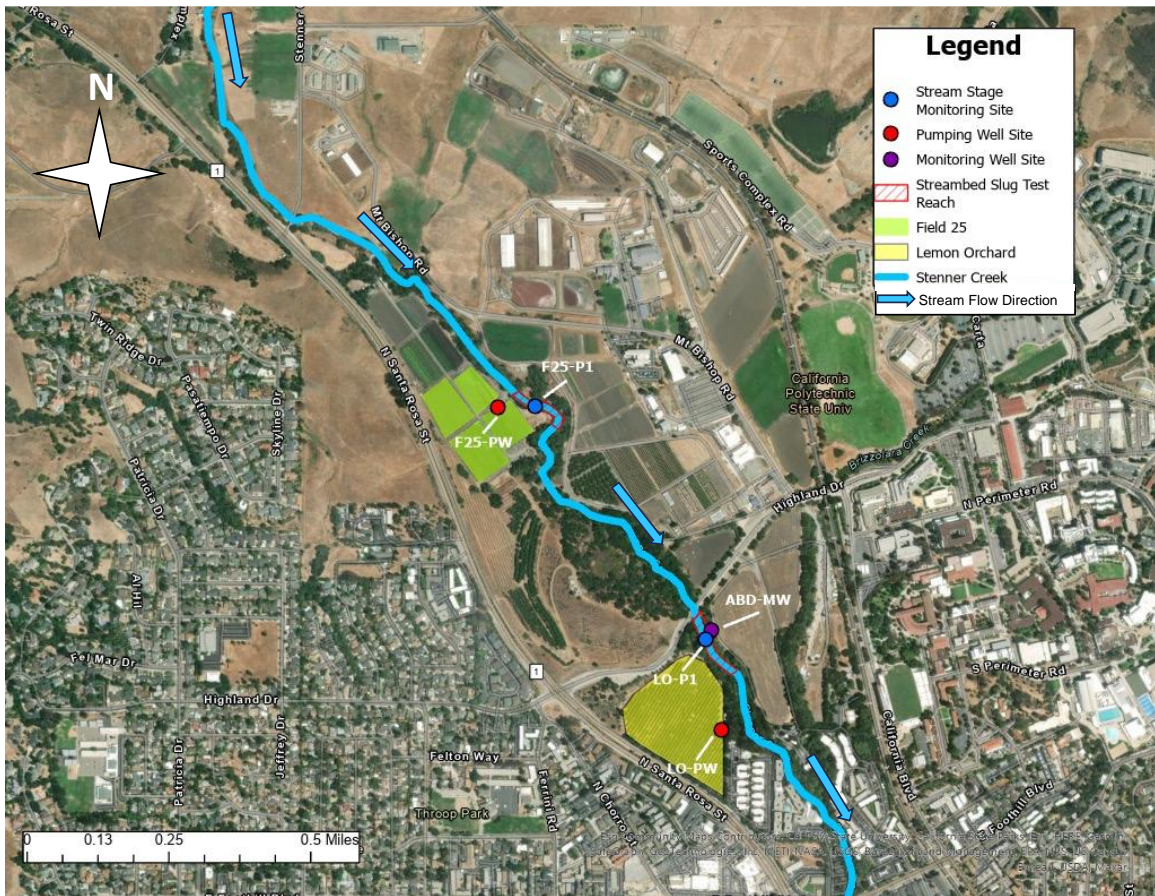


Figure 3.2 Overview map of Field 25 and Lemon Orchard pumping wells, monitoring wells, and in-stream piezometers.

3.2 Data Collection

Data collection in Steinner Creek included passive stream stage monitoring and active stream discharge measurements collected before, during, and after pumping within the subject agricultural wells. Aquifer water level data were gathered from the respective pumping and monitoring wells to detect when pumping occurs. The subsequent sections provide more detail on the data collection methods within Steinner Creek and the neighboring wells.

3.2.1. Passive Data Collection

The first portion of this study passively monitored the response of stream stage and aquifer water levels from August 2022 to August 2023 using SeaMetric PT2X pressure transducers with pressure readings expressed in pounds per square inch (psi).

3.2.1.1 Stream Stage Measurements

Two pressure transducers were installed in Stenner Creek, one located adjacent to the Lemon Orchard (“LO-P1”), and another located adjacent to Field 25 (“F25-P1”) as depicted in Figure 3.2 above. The stream stage monitoring locations were selected by identifying areas within the stream that were within the area of influence of the subject well, a penetrable streambed, and relatively deep to ensure stream stage data can be continuously collected without the risk of the stream stage measuring location turning dry in the summer months when stream discharge dwindles. F25-P1 was installed in the Spring of 2023 after the winter storms and prior to the commencement of seasonal pumping.

The two stream stage monitoring locations were installed by inserting a 6-ft. steel t-post into the sandy streambed and attaching a 2-in. polyvinyl-chloride (PVC) pipe apparatus. The PVC apparatus is comprised of 5-ft. perforated, 2-in. diameter PVC one-hundredth of an inch perforations located at the bottom of the PVC apparatus. The bottom of the PVC apparatus is completed with a point cap connected to the bottom of the perforated PVC portion. This PVC apparatus allows the transducer to rest on the stream bed and fill with water up to same height as the surrounding stream and protects the transducer from outside influences such as debris or animal tampering. The data collection port was secured to the upper bank of the stream and housed in a lockbox to protect the USB connector from wear-and-tear caused by the outdoor

environment. See Figure 3.3 for an image of the in-stream measurement apparatus at the Lemon Orchard and Field 25 locations.



Figure 3.3 Stream stage monitoring equipment and in-stream measuring sites.

Both in-stream transducers were programmed to record continuous pressure and temperature readings in five or fifteen-minute increments from August 2022 to August 2023 and April 2023 to August 2023 for LO-P1 and F25-P1, respectively. All data collection and transducer programming were performed using the software program Aqua4PLUS (SeaMetric, 2023). Aqua4PLUS is a communication software that enables communication with the transducer devices and allows data to be exported to a variety of different file formats. In this study, all data was exported to comma separated values (CSV) files and stored within Microsoft OneDrive to be shared amongst other researchers. As discussed in the results, some irregularities in the data were removed due to disturbances from animal tampering, historic wet weather, and flooding in Stenner Creek over the course of the 2023 winter.

3.2.1.2. Aquifer Water Level Measurements

The aquifer water level responses to pumping were continuously monitored with SeaMetric PT2X pressure transducers placed in each pumping well and two neighboring monitoring wells. The Lemon Orchard and Field 25 wells were selected based on the utilization rates of each well, the proximity to Stenner Creek, and accessibility. Field 25 is located upstream of the Lemon Orchard and is irrigated three to four days a week during dry months. The Lemon Orchard is located downstream of Field 25 and is irrigated for a duration of approximately 48-hours every two to three weeks depending on precipitation, atmospheric temperature, and evapotranspiration rates. Both irrigation wells have a uniform diameter of 8-in. and are each located approximately 200-ft. from Stenner Creek. The wells are completed through the entire thickness of the aquifer and are used to pump the confined aquifer depending on precipitation rates. The transducers are installed at a depth approximately at the interface between the top of the aquifer and the overlying clay confining unit. The data collected for this study was collected from August 2022 to August 2023 and April 2023 to August 2023 for the Lemon Orchard and Field 25, respectively.

3.2.2. Stream Discharge Measurements

Stream discharge measurements were taken in Stenner Creek in the direct vicinity of the stream stage sites prior to aquifer pumping, during aquifer pumping, and after pumping to observe fluctuations in stream discharges under the various pumping scenarios. Stream discharge was measured using the velocity-area method as per the USGS methodology with minor adjustments due to the study site limitations as mentioned in the Limitation section below. The measuring devices and tools used include a 100-ft. measuring tape graduated in decimal feet, two wooden stakes, two clamps, a hatchet (used to clear the cross-section and insert the wooden stakes), a 6-ft. streamflow rod (also in decimal feet), and an OTT MF pro - Water Flow Meter (the “discharge recording device”).



Figure 3.4 Stream discharge equipment and usage at the Lemon Orchard site.

The selected stream channel cross-sections were chosen based on the accessibility for installing the equipment and proximity to the stream stage recording location. The USGS volume-area method for measuring stream discharge requires that the segment of the stream being measured be five times the width of the stream (Turnipseed & Sauer, 2010). However, considering the meandering nature of Stenner Creek, the measurement section was measured to be only approximately three times the width of the stream. Since comparing the change in the measured stream discharge data under various pumping conditions are the subject of this portion of the study, it was determined that this shortcoming was negligible. Please see Section 3.6 for more detailed information on the limitations of this study.

The following steps were performed to measure the stream discharge in Stenner Creek using the velocity-area method with slight modifications based on the limitations of the study site. First, wooden stakes were installed on both the left and right banks of the stream with the “0” mark of the tape measure clamped to the wooden stake on the right side of the stream (when looking

down stream). The tape measure was then extended to the left bank and clamped to the other wooden stake located directly across the stream. The width of the stream at each cross-section was recorded for each discharge measurement data point collected. Ten, evenly spaced, measurement sites along the cross-section were identified and marked on the measuring tape. The stream flow rod and the water flow meter were used to record the stream depth and to collect 20-second average flow rate expressed in feet per second (fps) recordings at each of the ten marked sites. The flow measuring device collected data at each of sites along the cross-section at a depth 60% from the top of the water column (Turnipseed & Sauer, 2010). Once the stream flow data were collected, the streamflow measuring device computed the discharge of the stream expressed in cubic feet per second (cfs). The discharge rate, wetted width of the stream, and date and time were recorded for each discharge measurement collected in a field journal and inputted into a Microsoft Excel spreadsheet upon returning to the laboratory.

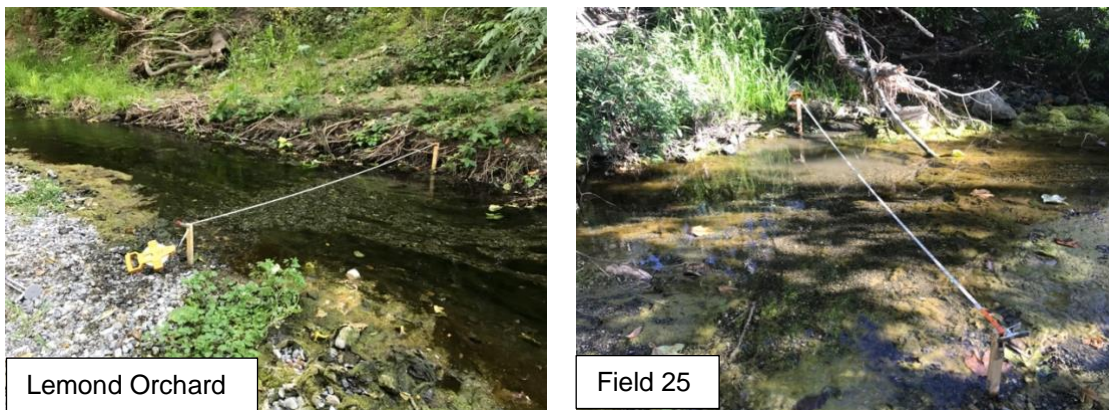


Figure 3.5 Stream discharge measuring locations at the Lemon Orchard and Field 25 sites.

Considering Field 25 is irrigated more frequently from the subject pumping well, stream discharge measurements were collected in Field 25 once in the morning the day of pumping (prior to pumping commencing), once during midday during pumping, and once in the afternoon after pumping was completed. In the case of the Lemon Orchard site, since pumping occurs less-frequently but for longer durations than Field 25, stream discharge measurements were collected two days prior to pumping with one discharge measurement per day leading up to the day of

pumping. Once pumping commenced, a discharge measurement was recorded in the morning and the afternoon of each day pumping occurred. After the multi-day pumping phase was completed, two discharge measurements were taken the day after pumping representing the discharge during as the stream recovers.

Pumping schedules were determined by communicating with the Cal Poly Agricultural Operations Department and based on prior pumping schedule tendencies. In total, 5 discharge measurements were recorded for Field 25 and 39 discharge measurements were recorded for the Lemon Orchard. The Field 25 location only produced five stream discharge measurements before the stream ran dry.

3.2.3. Streambed Conductivity Measurements

The third section of this study involves determining the hydraulic conductivity of the streambed to determine the hydraulic connectivity of the stream to the underlying aquifer system and the amount of storage within the stream channel, which influences the streambed's ability to store, transmit, and discharge water. This data is valuable for the time series analysis portion as it can help explain if there is an apparent connection between the aquifer and the stream and, if so, how the stream responds to aquifer pumping.

To determine the in-situ streambed conductivity, pneumatic slug tests were performed at nine locations upstream and nine locations downstream of the stream stage monitoring location for a total of eighteen locations selected for testing in the vicinity of the stream stage monitoring location. The furthest extents of the sampling reach started approximately 300-ft. upstream and approximately 300-ft. downstream of the P1 and Field 25 study sites as depicted in the figures below. Each studied reach of Stenner Creek was divided into upstream and downstream segments relative to the LO-P1 location with three zones tested within each segment. The

furthest tests were performed 300-ft. upstream and 300-ft. downstream of LO-P1 and the closest segments were performed within 6-ft. of LO-P1 location. Tests were also performed at the midpoint of the furthest and closest testing zones which are labeled as 150-ft. in the below table. The specific testing sites within each zone were selected based on the penetrability of the streambed, the location within the streambed cross-section (either banks or the center), and ability to stabilize the pressure within the well upon introduction of the slug. The procedures used for the streambed slug tests were based on the procedures used within Rus et al. (2001).

3.2.3.1. Well Site Selection

The in-stream well site was selected based on accessibility and ability to penetrate the streambed. Grain sizes within the streambed range significantly from fine silty soils to approximately 6-in. diameter impervious rocks and gravel. This resulted in nine slug test locations being identified in the vicinity of both LO-P1 and F25-P1 for a total of eighteen testing locations. However, as discussed in the data processing and limitations section below, some sites yielded unsuccessful tests due to various factors.

3.2.3.2. Well Installation

A manual direct-push method was used to install the streambed wells since the sediment was loosely packed and saturated. For areas with higher impenetrability, a pilot hole was created using a metal rod and a yard post driver to loosen the sediment and allow the well to be installed. The well that was used for the streambed conductivity testing is like the PCV casing for the stream stage monitoring apparatus. The well is comprised of a 5-ft. long, 1-in. diameter PVC pipe. The bottom 6-in. is comprised of PVC screen with one-hundredth of an inch perforations, adorned with a pointed cap to enable penetration into the streambed. The remaining 4.5-ft. of PVC is blank casing PVC and extends from the perforated portion to the top. The cap, screened, and blank casings were connected using PVC couplers. See Figure 3.6 below for an image of the apparatus and its corresponding parts.

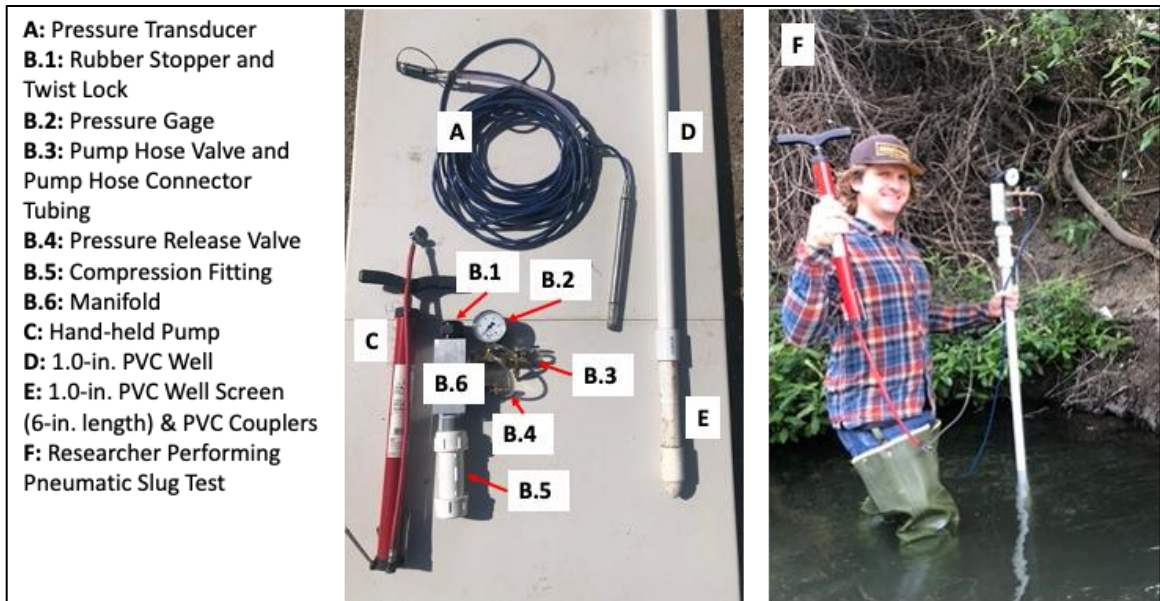


Figure 3.6 Streambed pneumatic slug test equipment and researcher using equipment.

As per Rus et al. (2001) the diameter of the well was selected to be 1-in. inch to prevent significant friction losses while also being small enough to reach the targeted depth of 8-in. below the streambed. It was assumed that there is no head loss from the movement of water between the casing and the screen (Rus et al., 2001). Once the well was constructed, an airtight manifold was attached to the top of the well and a SeaMetric PT2X pressure transducer was installed and programmed to record pressure readings every second for the duration of testing at each location. The airtight manifold is comprised of connector tubing, a #5 stopper and clamp, an air valve and connector tubing, and a pressure gauge graduated in increments of 5 in-H₂O of water up to 100 in-H₂O.

3.2.3.3 Well Development

Once the well installed to 8-in. below the streambed surface, the film of silty material that developed around the screen with low-K was removed to unclog the screen. This involved

performing 20 vigorous strokes to remove the low-K material. Continuous monitoring of the real-time data allowed us to see when adequate displacement occurred and the recovery of the water level (Rus et al., 2001).

3.2.3.4. Performing Pneumatic Slug Tests

Once the well is installed and sealed with an airtight manifold, a hand pump was attached to inject air into the well casing. This pressurization of air within the well displaced the water thereby lowering the water level from static. The pressure in the well casing was monitored using a pressure gage that graduated in units of 5 in-H₂O. The air pressure injected inside the well was adjusted until the gage read a pressure identical to the targeted initial displacement of between 5 and 10 in-H₂O. After the desired pressure in the well was achieved and stabilized, a quick release valve on the manifold was opened to depressurize the system and let the water permeate back into the well (Rus et al., 2001). The recovery of the water level from initial displacement back to static level is the relevant data for each test. This process was performed three times at each location.



Figure 3.7 Map of the Lemon Orchard study site.

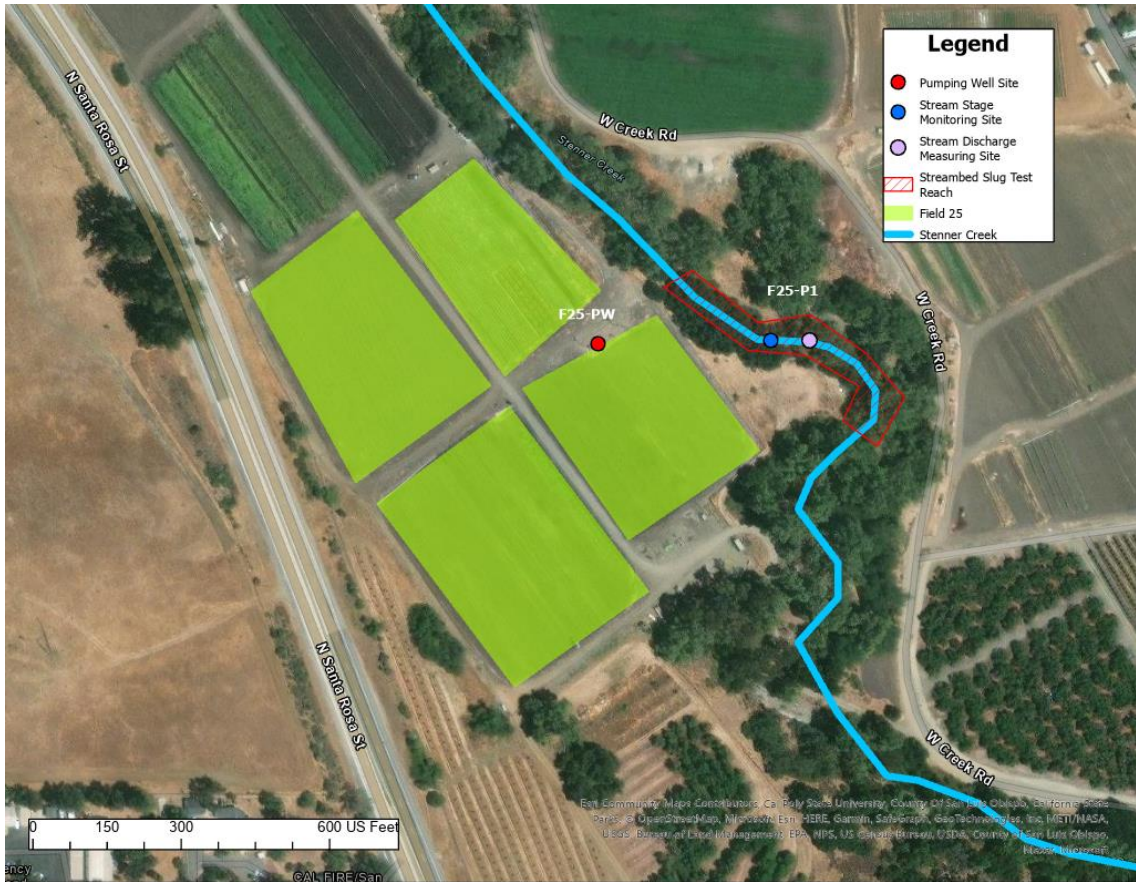


Figure 3.8 Map of the Field 25 study site.

3.3 Stream Stage and Aquifer Water Level Data Analysis

The stream stage data and aquifer water level datasets were downloaded from their respective transducers and exported to CSV files. These files were collected from the transducers bi-weekly throughout the duration of the study (Aug. 2022 – Aug. 2023). The exported CSV files list the pressure readings in psi and the time of recording. Once the stream stage and groundwater data were collected, the raw data of each corresponding stream stage and groundwater datasets were plotted using Microsoft Excel’s scatter plot function, which created a scatter plot of both times series represented as pressure, represented in psi, on the y-axis and the time of recording, represented in seconds, on the x-axis. The stream stage and aquifer data were plotted on the same chart with two y-axes (one representing the stream stage and the other representing the

aquifer water level) to identify when pumping occurred in the well and if there were any subsequent visible declines in stream stage. Pumping in each well is detectable in the raw data when the pressure above the transducer drops abruptly from the static water level. This indicates an instantaneous drop in the water level caused by the commencement of pumping. When the pumping event was completed, the water level recovered slowly of the pre-pumping water level.

The initiation of observable drawdown and the initiation of observable recovery in stream stage and water level were detected using various Microsoft Excel functions in addition to visually identify the relevant points on the plotted data series. The date, time, and water level or stream stage, at drawdown initiation and recovery were recorded which allowed us to identify the duration of drawdown, represented in hours, and the amount of drawdown detected, represented in feet.

Plotting the stream stage data and corresponding groundwater data on the same chart also allowed us to identify visible declines in stream stage beyond of the cyclic nature of stream stage. For example, a common cyclic factor that can influence stream stage data is evapotranspiration (ET) during the daylight hours and in the summer months when discharge dwindles (Lundquist & Cayan, 2002). Additionally, trends in the data such as annual stream stage decline during drier months needed to be accounted for when analyzing the dataset to avoid incorrectly attributing a greater magnitude of groundwater pumping on stream stage decline. Lastly, human tampering, device disruption, and changes in water levels due to debris falling into the stream and disrupting the stream stage data collection, referred to as “noise”, needed to be corrected for within the stream stage dataset (Malama et al., 2021).

In order to correct for cyclic trends in the stream stage data and remove any external noise that could distort the attributable effects of groundwater pumping on stream stage, the stream stage and aquifer water level time series datasets were detrended and denoised through a cyclic signal

analysis, specifically, a Fast-Fourier Transform (FFT) (Cooley & Tukey, 1965). This analysis allowed us to identify the frequency of cycles within the stream stage and aquifer water level data due to biweekly pumping, daily trends such as evapotranspiration, and other influences. Once the raw stream stage and aquifer data was corrected for noise and trends, a spectral analysis was performed to compare the fluctuations within the stream stage and aquifer water level data to determine if the observed drawdown corresponds to aquifer pumping. Each spectral analysis figure (presented in the Results Chapter) depicts the raw data, the detrended data, the reconstructed data (reconstructed using an inverse FFT after discarding minor frequency components), the reconstructed data plotted with the detrended dataset, the residuals (represented as the difference between the detrended data and the reconstructed data), and a bar chart displaying the major and minor power spectrum densities. The power spectrum density threshold, which defines major and minor signals, was adjusted for each dataset to isolate, and classify major signals appropriately.

3.4 Stream Discharge Data Analysis

Theis (1941) concluded that pumping from a connected aquifer is likely to diminish stream discharge. The goal of the stream discharge analysis is to determine if there is any relationship between the measured stream discharge and stream stage in Stenner Creek and to identify if certain discharge rates validate or invalidate the constant head boundary assumption.

The stream discharge data recorded contains measurements of the Stenner Creek discharge rate before aquifer pumping, during aquifer pumping, and after aquifer pumping at the Lemon Orchard and Field 25 locations. The stream discharge measurements were recorded directly next to the stream stage measuring locations. See Figure 3.7 and Figure 3.8 above for a depiction of the stream discharge and stream stage measuring locations. The data that was collected and calculated with the stream discharge device was entered manually into a Microsoft Excel file.

In order to identify relationships between the stream discharge rate and stream stage, the discharge data was plotted on a line-plot using Microsoft Excel and compared to the relevant aquifer water level data. This allowed us to observe any trends in the measured stream discharge rates relative to aquifer pumping phase, which was detectable using the aquifer water levels at the Lemon Orchard and Field 25 locations. The stream discharge and aquifer water level data were analyzed qualitatively based on the line-plots developed for each time series. The observed trends in stream discharge were then used to frame the findings of the stream stage analysis as discussed further in the Results and Discussion chapters.

3.5 Streambed Conductivity Data Analysis

The data gathered from pneumatic slug tests within the streambed of Stenner Creek were exported from the transducer into a CSV file. The corresponding data for each location was labeled accordingly during data collection. Similar to the stream drawdown data processing, the slug tests were detected by identifying the visible drops in the well's static water level. These drops in water levels within the well indicate the displacement of water due to the injection of air, and the subsequent water level recovery back to static was extracted for each slug test cycle. Each slug test was then copied and pasted into a separate CSV file for each slug test location and labeled accordingly. See Figure 3.9 for a depiction of the raw data and the highlighted areas showing the displacement from the pneumatic slug and water level recovery in the streambed well. Once each individual slug test data was extracted from the raw data, the pressure data (represented in psi) was converted to displacement data expressed in feet. See Figure 3.10 below showing a scatter plot of the displacement data derived from the process described above. This procedure of converting the raw data into displacement data was performed for each slug test sequence at each location using Microsoft Excel functions. Once each slug test was extracted and processed correctly, the displacement data were exported AQTESOLV v4.5 to perform conductivity calculations.

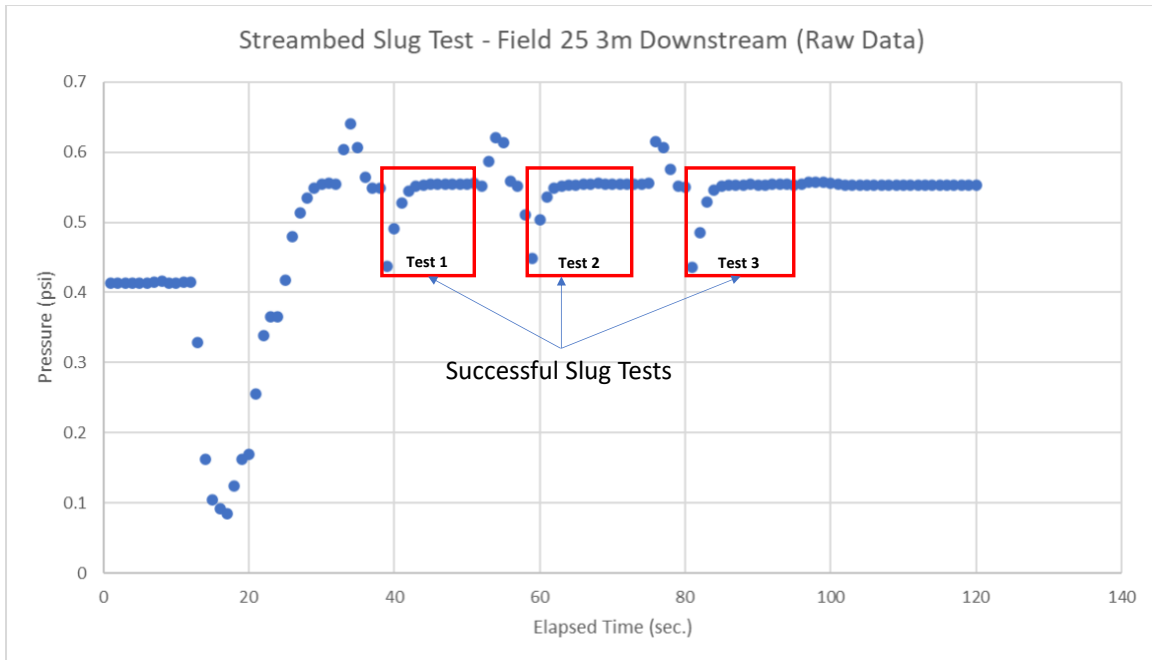


Figure 3.9 Example of streambed slug test raw data in a scatter plot.

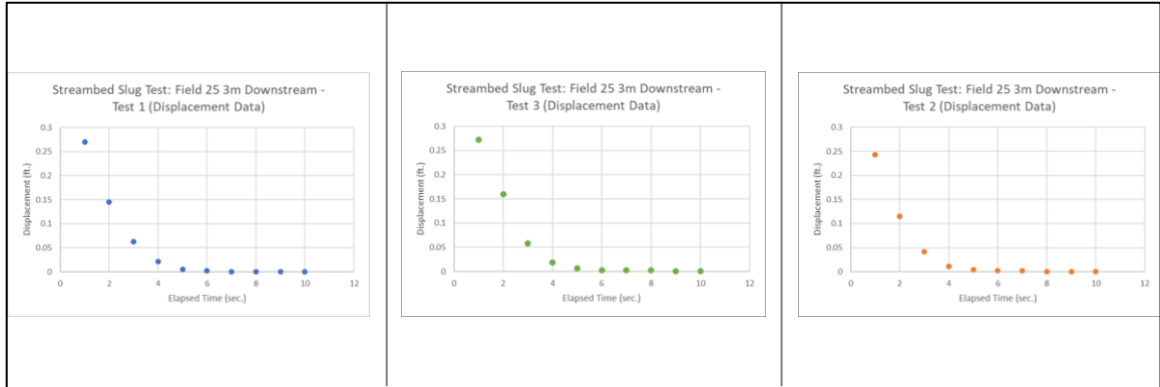


Figure 3.10 Example of extracted streambed slug test displacement scatter plots to be used in AQTESOLV.

AQTESOLV is an advanced aquifer test and analysis software that calculates hydraulic conductivity with a variety of methods. The method utilized for the streambed conductivity analysis within AQTESOLV was Hvorslev (1951). The parameters used within the AQTESOLV are stated in Table 3.1 below. The Hvorslev (1951) method was selected because of the

streambed being classified as a shallow unconfined aquifer for analysis purposes. Each conductivity measurement was mapped and input into a table, as shown in the Results chapter below. Identifying the conductivity of the streambed provides a more complete picture of the observed stream stage and stream discharge data in relation to aquifer pumping. The results of the streambed pneumatic slugs are presented in the results section below.

Table 3.1 AQTESOLV Input Format

AQTESOLV INPUTS	
Ag. Field (Lemon Orchard or Field 25)	<Insert Data>
Reach (Up = Upstream, Down = Downstream)	<Insert Data>
Segment (300 ft., 150 ft., or 6ft.)	<Insert Data>
Position in Stream (Left, Right Middle)	<Insert Data>
AQTESOLV Parameters	
H(0): Observed Initial Displacement (ft.)	<Insert Data>
H (Static water column height) (ft.)	<Insert Data>
Well Name	<Insert Data>
Saturated Thickness of Aquifer (ft.)	<Calculated>
Kv/Kh (Vert to Horz K ratio.)	<Calculated>
Depth to Top of Well Screen (ft.)	<Calculated>
Length of Well Screen	<Calculated>
Transducer depth (ft.)	<Calculated>
Relevant Radii (Same for All Tests)	
r(c) - inside radius of well casing (ft.)	0.041667
r(eq) - radius of downhole equip (transducer) (ft.)	0.031266
r(p) - radius of packer (ft.)	0.00001
r(w) - radius of well (ft.)	0.041667
r(sk) - radius of outer well skin (ft.)	0.041677
*Don't apply Effective Casing Radius Data	
AQTESOLV Results	
Method: Hvorslev Method (Unconfined)	
Calculated Conductance (K) (ft/s)	<Insert Calculated Value from AQTESOLV>

Key	
<Insert Data>	Input values
<Calculated>	Calculated values from inputs

3.6 Limitations

During the passive monitoring of stream stage, there are a variety of disturbances to the data collecting process due to natural and anthropogenic effects. For example, significant rain events in January 2023 caused flooding and bank erosion within Stenner Creek, which resulted in the relocation of transducer devices from their original posts due to debris and erosion of the bank where the lockbox was located. Additionally, human tampering with the transducers and the water

within the collection site during passive data collection caused disruptions or “noise” within the collected data that needed to be corrected prior to analysis. Additionally, site access was also a limiting factor and a key contributor to the sites selected for the passive stream stage monitoring process.

The limitations within the stream discharge recordings are the frequency of discharge recordings due to equipment and personnel limitations. Ideally, having a method to passively monitoring stream discharge would allow the continuous collection of discharge data which could be compared to the stream stage data collected. Although collecting discharge measurements daily for non-pumping and twice per-day during pumping provides an overview of the change in discharge rates, it does not provide the same granularity as the stream stage data. Additionally, due to the size and the meandering nature of Stenner Creek, it was not possible to find a segment of Stenner Creek that follows the USGS Volume Area recommendation of the length of the stream reach be five-times the width of the measured cross-section (Turnipseed & Sauer, 2010). This shortcoming was determined to be negligible since this study is concerned with the change in measured discharge as opposed to the quantity of discharge. Therefore, consistency in the method used throughout the data collection process was determined to be most important. Also, the stream ran dry at the Field 25 location after only five stream discharge measurements were recorded due to the progression of the dry summer months and continuous aquifer pumping. Finally, since this study did not have control of the pumping schedule from the subject wells, it was not always possible to collect discharge data at the desired time. It is recommended that future researchers either operate the pumping well directly or with consistent communication with the well operators.

The streambed conductivity testing was limited to the use of a transducer programmed to collect records every second, as opposed to a transmitter and data logger which has the capability to record datapoints in tenths of a second. The streambed conductivity calculations using

AQTESOLV could have been more accurate using a transmitter since the transmitter can provide ten datapoints to the transducers one datapoint. As discussed in the Results chapter, certain slug tests only provided three data points which was determined to be inadequate for calculating accurate stream conductivity values. The transmitter equipment required to perform these tests was too heavy to carry into the streambed for one person, so the transducer method was determined to be the only feasible option for this Project. The selection of each slug test location within the streambed was also limited to the penetrability of the streambed as some areas were impenetrable due to high concentrations of gravel or solid rock within the streambed.

CHAPTER 4: RESULTS

4.1 Stream Stage Response to Aquifer Pumping

The results from the passive stream stage data time series analysis showed a varied relationship between aquifer pumping and stream stage drawdown. The main differentiator at the Lemon Orchard site was the Dry Season in which the data was collected and the associated discharge rates, as discussed in more detail in the Discussion section. Field 25 was monitored after the 2022-2023 Wet Season and therefore seasonal changes were not identifiable within the Field 25 stream stage and aquifer water level time series and spectral analyses.

4.1.1 Time Series Analysis of Stream Stage and Aquifer Water Levels at the Lemon Orchard Site

The Lemon Orchard was irrigated for approximately 48-hours every two weeks during the 2022 and 2023 Dry Seasons with intermittent minor pumping events. The stream stage and aquifer water level data in the Lemon Orchard collected from August 2022 to August 2023 can be classified into three categories: 2022 Dry Season, 2022/2023 Wet Season, and 2023 Dry Season. The 2022 and 2023 Dry Seasons are identified in Figure 4.1 by the relatively stagnant water levels with sudden drops in the aquifer water levels measured in ABD-MW and LO-PW indicating aquifer pumping occurred. The 2022-2023 Wet Season is identified by the spikes in stream stage and aquifer water levels, indicating precipitation events and associated recharge of the aquifer-stream system, followed by steady decline as the groundwater and stream flow is discharged down gradient. In the 2022 Dry Season, the drawdown observed within the stream and aquifer, due to aquifer pumping, are followed by relatively slow recovery of the aquifer water level and stream stage in ABD-MW and LO-P1, respectively. This is a result of lower quantities of surface and subsurface discharge associated with the later months of summer and fall when precipitation is infrequent. The stream stage and aquifer water levels observed in the 2023 Dry Season displayed faster recovery due to higher surface and subsurface discharge rates.

We did not install a pressure transducer in LO-PW to record aquifer water level data during the 2022 Dry Season and, therefore do not know definitively when pumping began in LO-PW during the 2022 Dry Season. However, based on 2023 Dry Season observations in LO-PW and ABD-MW, we know that aquifer pumping from LO-PW is detected by the observed drawdown within ABD-MW. Additionally, the 2023 January rain events damaged LO-P1, buried it in debris and transplanted the device downstream of the original location. After retrieving, repairing, and re-installing the LO-P1 transducer, LO-P1 was removed prior to expected high precipitation events to avoid further damages and potential data loss. The LO-P1 values at and around “0” in Figure 4.1 indicate when LO-P1 was removed from the stream to prevent further damage from high discharge and associated debris.

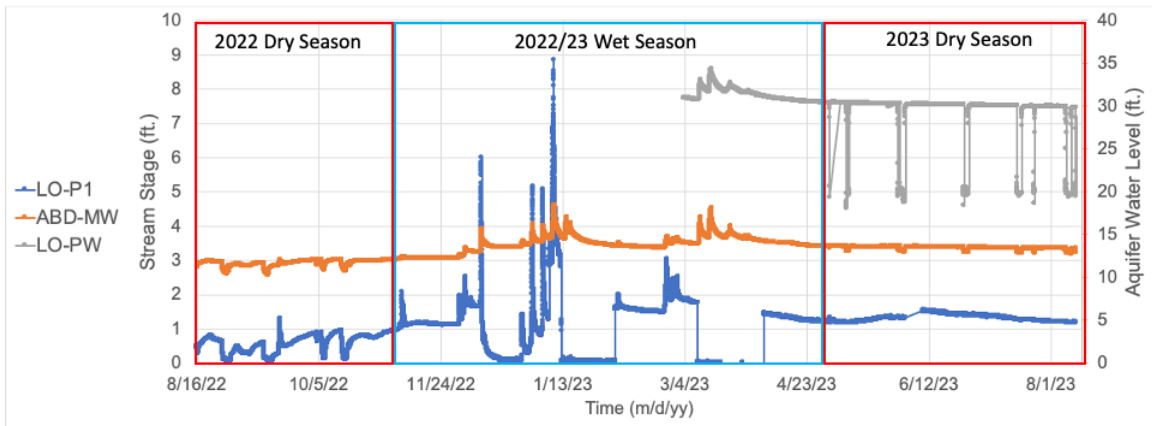


Figure 4.1 Stream stage and aquifer water levels from Aug. 2022 to Aug. 2023 at Lemon Orchard site.

Focusing on the 2022 Dry Season and associated pumping events, we see a similar response in stream stage at LO-P1 compared to the aquifer water level observed within ABD-MW during aquifer pumping. When pumping occurs in LO-PW, the stream stage, as observed in LO-P1, and aquifer water levels, observed in ABD-MW, exhibit sharp declines when pumping begins and slow recovery once pumping is complete. Figure 4.2 depicts the 2022 Dry Season stream stage and aquifer water levels with the y-axes adjusted to show the similar relationship between stream stage and aquifer water level responses to aquifer pumping. The pumping events are boxed in grey and numbered chronologically.

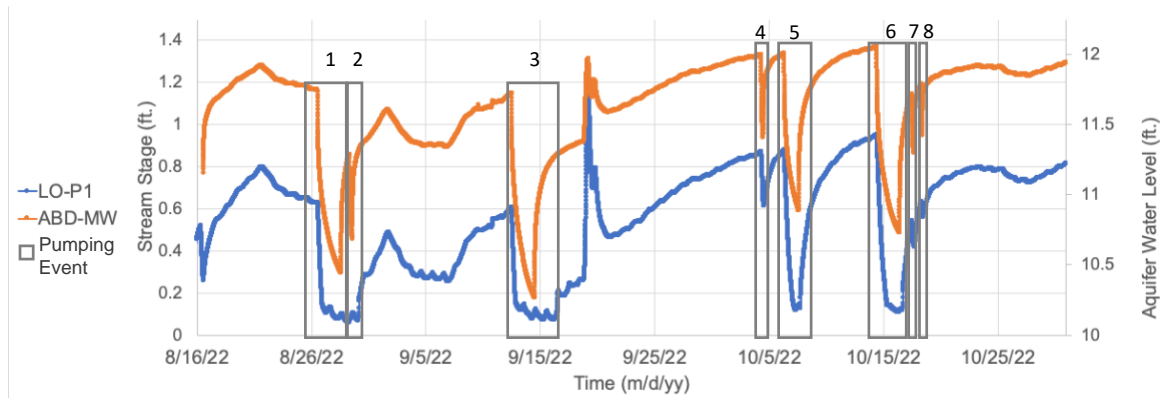


Figure 4.2 Stenner Creek stream stage and aquifer water level at Lemon Orchard site during 2022 Dry Season with pumping events identified.

Table 4.1 and Table 4.2 list the date and time of the observed initial drawdown and the initial recovery associated with each pumping event within ABD-MW and LO-P1. Generally, the observed drawdown in LO-P1 were of longer duration than the drawdown observed in ABD-MW; however, after Pumping Event 5 the stream stage in LO-P1 began to recover sooner than in ABD-MW. In ABD-MW, the longest observed drawdown duration occurred in Pumping Event 1 which lasted approximately 49 hours and resulted in 1.303-ft. of drawdown within the monitoring well. The shortest observed drawdown duration in ABD-MW occurred in Pumping Event 8 which lasted approximately 1.5 hours and resulted in 0.358-ft. of drawdown. Drawdown observed within ABD-MW ranged from 0.358-ft. to 1.462-ft. which occurred in Pumping Events 8 and 3, respectively. In LO-P1, the longest observed drawdown duration occurred in Pumping Event 1 which lasted approximately 49 hours and resulted in 0.531-ft. of drawdown within the stream. The shortest observed drawdown duration in LO-P1 occurred in Pumping Event 8 which lasted approximately 1.5 hours and resulted in 0.072-ft. of drawdown. Drawdown observed in LO-P1 ranged from 0.072-ft. to 0.839-ft. occurring in Pumping Events 8 and 6, respectively.

A rain event occurred on 9/19/2022, depicted by the spike in stream stage and aquifer water levels in LO-P1 and ABD-MW, respectively. This precipitation event provided recharge to the aquifer-stream system as exhibited by the general increase in stream stage and aquifer water levels in LO-P1 and ABD-MW, respectively, after the 9/19/2022 precipitation event. Additionally, the stream and aquifer exhibited faster recovery rates when compared to the recovery rates prior to the 9/19/2022 precipitation event due to higher surface and subsurface discharge rates.

Table 4.1 Maximum observable drawdown duration and quantity in the aquifer at ABD-MW during 2022 Dry Season pumping events.

ABD-MW						
Pumping Event No.	Date/Time (m/d/yy hh:mm)			Water Level (ft.)		
	Initial Drawdown Observed	Initial Recovery Observed	Max. Drawdown Duration (hours)	Initial Drawdown Observed	Initial Recovery Observed	Max. Observed Drawdown (ft.)
1	8/26/22 13:40	8/28/22 14:45	49.1	11.742	10.439	1.303
2	8/29/22 8:30	8/29/22 14:25	5.9	11.284	10.684	0.601
3	9/12/22 12:30	9/14/22 13:00	48.5	11.723	10.261	1.462
4	10/4/22 8:30	10/4/22 13:00	4.5	11.987	11.407	0.580
5	10/6/22 8:45	10/7/22 15:15	30.5	12.003	10.887	1.116
6	10/14/22 10:55	10/16/22 10:40	47.8	12.054	10.728	1.326
7	10/17/22 12:50	10/17/22 17:10	4.3	11.714	11.294	0.420
8	10/18/22 9:10	10/18/22 10:45	1.6	11.783	11.425	0.358

Table 4.2 Maximum observable drawdown duration and quantity in Stenner Creek at LO-P1 during 2022 Dry Season pumping events.

LO-P1						
Pumping Event No.	Date/Time (m/d/yy hh:mm)			Stream Stage (ft.)		
	Initial Drawdown Observed	Initial Recovery Observed	Max. Drawdown Duration (hours)	Initial Drawdown Observed	Initial Recovery Observed	Max. Observed Drawdown (ft.)
1	8/26/22 13:45	8/28/22 14:45	49.0	0.626	0.095	0.531
2	8/29/22 8:30	8/29/22 14:25	5.9	0.062	0.097	0.000
3	9/12/22 12:40	9/14/22 13:00	48.3	0.605	0.099	0.506
4	10/4/22 8:30	10/4/22 14:30	6.0	0.871	0.612	0.259
5	10/6/22 8:55	10/7/22 11:05	26.2	0.878	0.120	0.758
6	10/14/22 11:05	10/16/22 11:00	47.9	0.949	0.111	0.839
7	10/17/22 13:15	10/17/22 18:15	5.0	0.541	0.418	0.122
8	10/18/22 9:20	10/18/22 12:25	3.1	0.631	0.559	0.072

A total of ten pumping events occurred during the 2023 Dry Season data collection period. These pumping events varied in duration with shorter pumping events generally occurring earlier in the season and longer pumping events beginning on 5/31/2023 and continued based on a biweekly schedule until the final data collection event. The drawdown due to pumping observed within ABD-MW is detectable by the corresponding dips in the aquifer water level when compared to the LO-PW data. Drawdown within Stenner Creek at LO-P1 was not as easily observed during the 2023 Dry Season as it was during the 2022 Dry Season. Some drawdown in stream stage is observed in LO-P1 during Pumping Events 7 and 9, as depicted in Figure 4.3, which were the longest duration at the latter half of the 2023 Dry Season when discharge was lowest during the data collection period. More information regarding the potential reason for this is discussed in the subsequent Discussion chapter. The main observable fluctuations in the stream stage time series data appear to be diurnal, depicted in Figure 4.3 below, which show higher stream stage values during the night and early morning, when atmospheric temperatures are lowest, and lower stream stage values during the midday and later afternoon, when atmospheric temperatures are highest. As discussed in the Discussion chapter, this is likely due to evapotranspiration (ET).

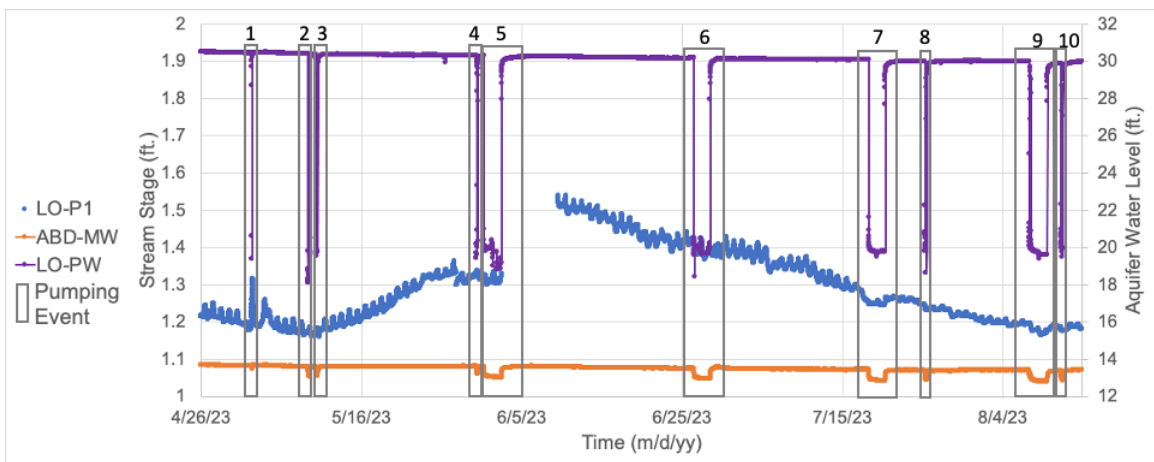


Figure 4.3 Stenner Creek stream stage and aquifer water level at Lemon Orchard site during 2023 Dry Season with pumping events identified.

In ABD-MW, the longest observed drawdown duration during the 2023 Dry Season occurred in Pumping Event 9 which lasted approximately 54.5 hours and resulted in 0.617-ft. of drawdown in the monitoring well. The shortest observed drawdown duration in ABD-MW during the 2023 Dry Season occurred in Pumping Event 1, which lasted approximately 0.8 hours and resulted in 0.196-ft. of drawdown. The drawdown observed within ABD-MW ranged from 0.196-ft. to 0.626-ft. occurring in Pumping Events 1 and 5, respectively. There was no significant drawdown observed in LO-P1 during the 2023 Dry Season as was observed during the 2022 Dry Season time series analysis at the Lemon Orchard site. However, there was minor stream drawdown observed in the latter pumping events 7 and 9 during the 2023 Dry Season characterized by the diminishing diurnal fluctuations.

Table 4.3 Maximum observable drawdown duration and quantity in aquifer at ABD-MW during 2023 Dry Season pumping events.

ABD-MW						
Pumping Event No.	Date/Time (m/d/yy hh:mm)			Water Level (ft.)		
	Initial Drawdown Observed	Initial Recovery Observed	Max. Drawdown Duration (hours)	Initial Drawdown Observed	Initial Recovery Observed	Max. Observed Drawdown (ft.)
1	5/2/23 9:00	5/2/23 9:45	0.8	13.645	13.449	0.196
2	5/9/23 9:15	5/9/23 14:15	5.0	13.580	13.058	0.522
3	5/10/23 9:45	5/10/23 15:00	5.3	13.560	13.075	0.485
4	5/30/23 10:00	5/30/23 11:30	1.5	13.592	13.197	0.395
5	5/31/23 8:00	6/2/23 11:00	51.0	13.587	12.961	0.626
6	6/26/23 13:15	6/28/23 12:00	46.7	13.477	12.934	0.543
7	7/18/23 8:00	7/20/23 10:00	50.0	13.419	12.821	0.598
8	7/25/23 9:00	7/25/23 15:15	6.2	13.368	12.860	0.508
9	8/7/23 9:30	8/9/23 16:00	54.5	13.375	12.758	0.617
10	8/11/23 8:45	8/11/23 15:15	6.5	13.347	12.851	0.497

4.1.2 Spectral Analysis of Stream Stage and Aquifer Water Levels at the Lemon Orchard Site

The results of the spectral analysis for the LO-P1 and ABD-MW data collected for the 2022 Dry Season, as shown in Figure 4.4 and Figure 4.5, respectively, show stronger signals at lower

frequencies of 0.10 cycles per day (cpd) and below. Considering aquifer pumping occurred approximately every two weeks (0.07 cpd), the cluster of signals at 0.10 cpd and below are therefore attributed to aquifer pumping. The power spectrum density (PSD) threshold used to define major and minor signals for the 2022 Dry Season was $PSD > 1.5 \text{ ft.}^2$ and $PSD > 5.0 \text{ ft.}^2$ for LO-P1 and ABD-MW, respectively. The diurnal and semidiurnal effects are negligible in both datasets because the PSD were below the major and minor signal threshold. This means aquifer pumping had an overwhelmingly strong influence on the collected data for both LO-P1 and ABD-MW. Diurnal and semidiurnal influences on stream stage and aquifer water level data are discussed further in the Discussion chapter.

Due to the gap in data collection at LO-P1 from 6/2/2023, to 6/9/2023, the spectral analysis for the 2023 Dry Season was separated into two time periods and labeled accordingly. The spectral analysis for the LO-P1 and ABD-MW data collected for the first part of the 2023 Dry Season (4/26/2023 to 6/2/2023) are shown in Figure 4.6 and Figure 4.7, respectively. The PSD threshold used to define major and minor signals was $PSD > 0.005 \text{ ft.}^2$ and $PSD > 0.1 \text{ ft.}^2$ for LO-P1 and ABD-MW, respectively. These figures show stronger diurnal and semidiurnal signals, at 1 cpd and 2 cpd, respectively, during the subject period which corresponds to higher discharge rates recorded within the stream. LO-P1 (Figure 4.6) did not display as strong of signals at 0.10 cpd and below during the period from 4/26 to 6/2 when compared to the 2022 Dry Season spectral analysis. This indicates that aquifer pumping did not have as strong of an influence on the collected stream stage data at LO-P1 during this period but could have an underlying influence that was not observed during the time series analysis. This is further verified by the ABD-MW (Figure 4.7) spectral analysis for the data collected from 4/26/2023 to 6/2/2023 which continued to detect strong signals at 0.10 cpd and below similar to the ABD-MW 2022 Dry Season data (Figure 4.5). The similarities between the spectral analysis of the data collected in ABD-MW for 2022 and 2023 Dry Season indicate that pumping continued to have an impact on the collected data within ABD-MW during the 2023 Dry Season, although it was not as easily observable during the time series analysis.

The spectral analysis for the data gathered at LO-P1 during the latter half of the 2023 Dry Season (6/9/2023 to 8/14/2023), Figure 4.8, shows stronger diurnal trends as the climate shifted towards the drier and hotter summer months. The spectral analysis for the data gathered at ABD-MW during the latter half of the 2023 pumping season (6/9/2023 to 8/14/2023), Figure 4.9, continued to contain stronger signals at lower frequencies which are attributed to bi-weekly aquifer pumping with no major diurnal nor semidiurnal signals detected. LO-P1 (Figure 4.8) also contained a higher semidiurnal signal than the earlier 2023 Dry Season data (Figure 4.6). LO-P1 also contained major signals at 0.10 cpd and below during the latter half of the 2023 Dry Season (Figure 4.8) which could be attributed to aquifer pumping. The PSD threshold used to define major and minor signals for the data gathered between 6/9/2023 to 8/14/2023 was $\text{PSD} > 0.005 \text{ ft.}^2$ and $\text{PSD} > 1.0 \text{ ft.}^2$ for LO-P1 and ABD-MW, respectively.

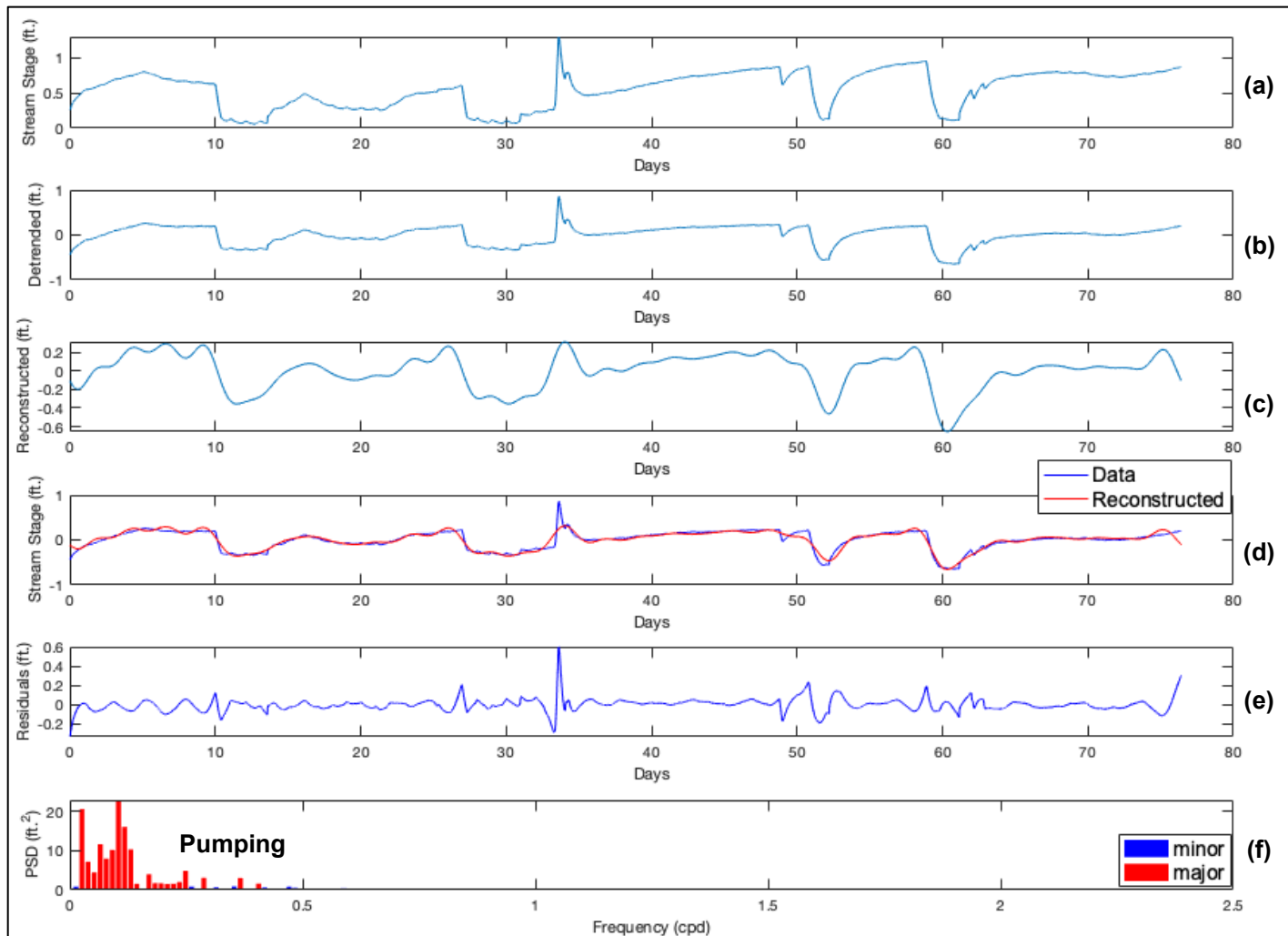


Figure 4.4 Spectral analysis of LO-P1 for 2022 Dry Season. Respectively, a) raw data, b) raw data detrended, c) reconstructed data with cubic polynomial fit, d) reconstructed and detrended data, e) residuals represented as difference between reconstructed and detrended data, and f) power spectra with frequencies with major and minor signals identified.

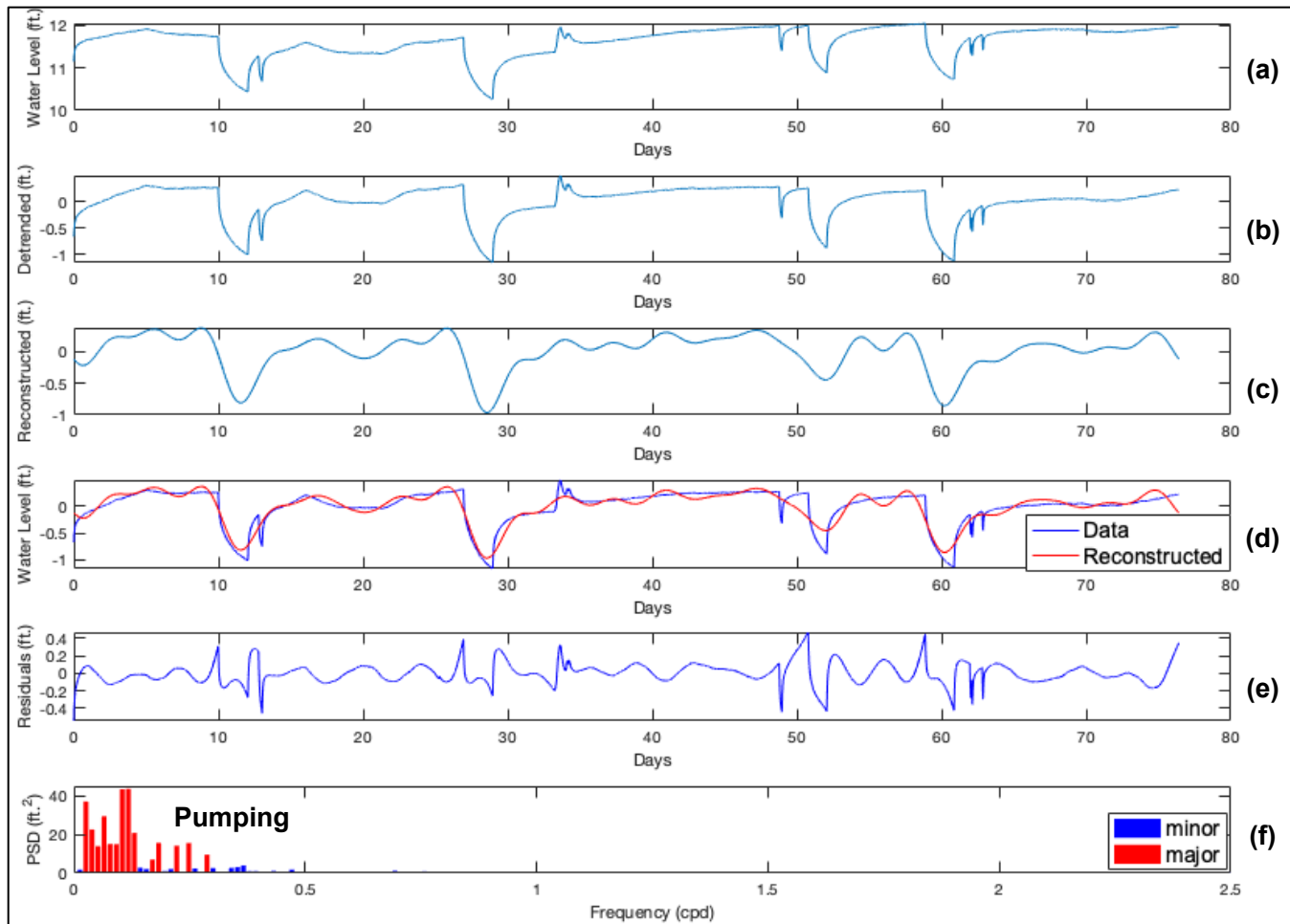


Figure 4.5 Spectral analysis of ABD-MW for 2022 Dry Season. Respectively, a) raw data, b) raw data detrended, c) reconstructed data with cubic polynomial fit, d) reconstructed and detrended data, e) residuals represented as difference between reconstructed and detrended data, and f) power spectra with frequencies with major and minor signals identified.

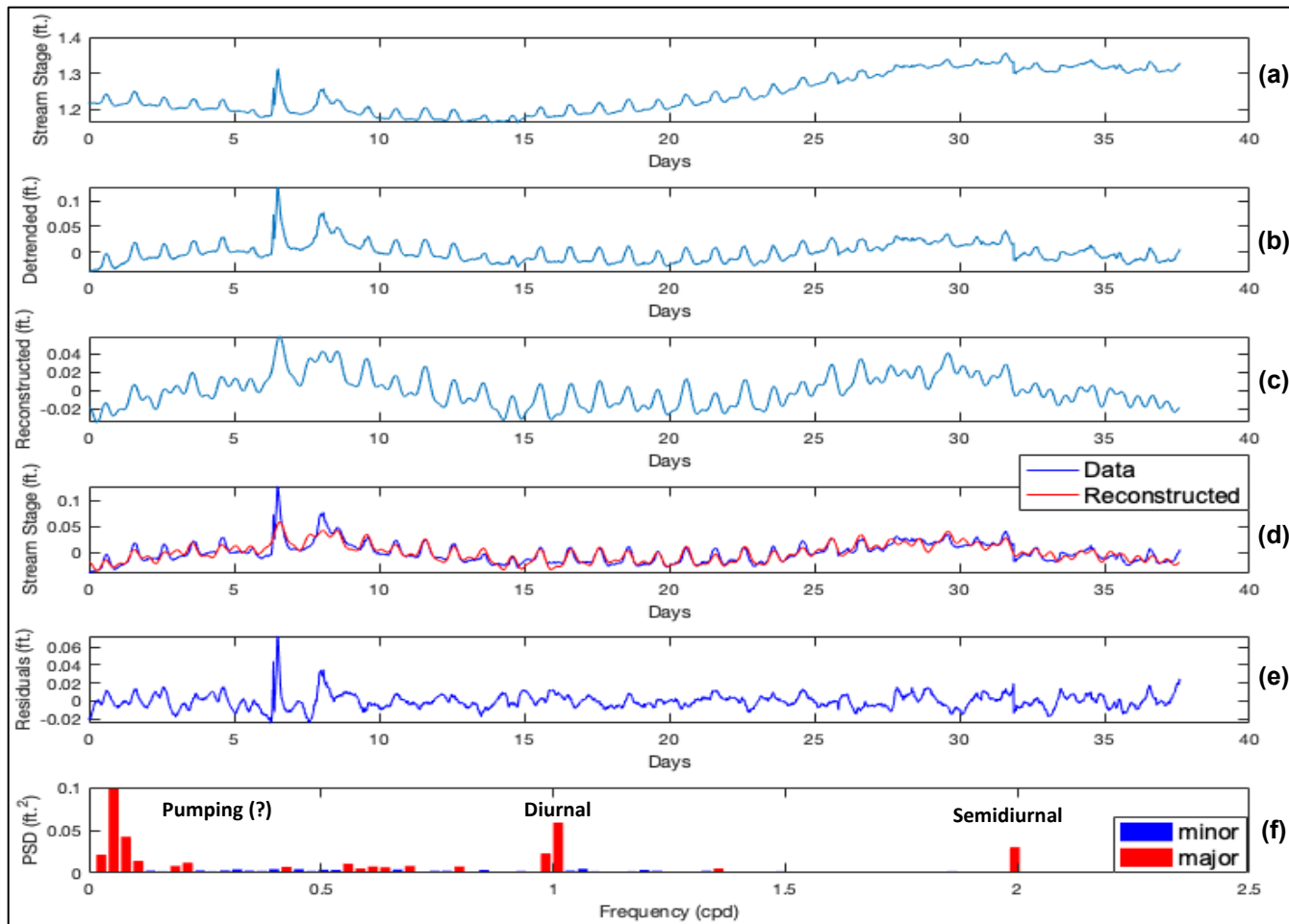


Figure 4.6 Spectral analysis of LO-P1 for 2023 Dry Season from April 26 to June 2. Respectively, a) raw data, b) raw data detrended, c) reconstructed data with cubic polynomial fit, d) reconstructed and detrended data, e) residuals represented as difference between reconstructed and detrended data, and f) power spectra with frequencies with major and minor signals identified.

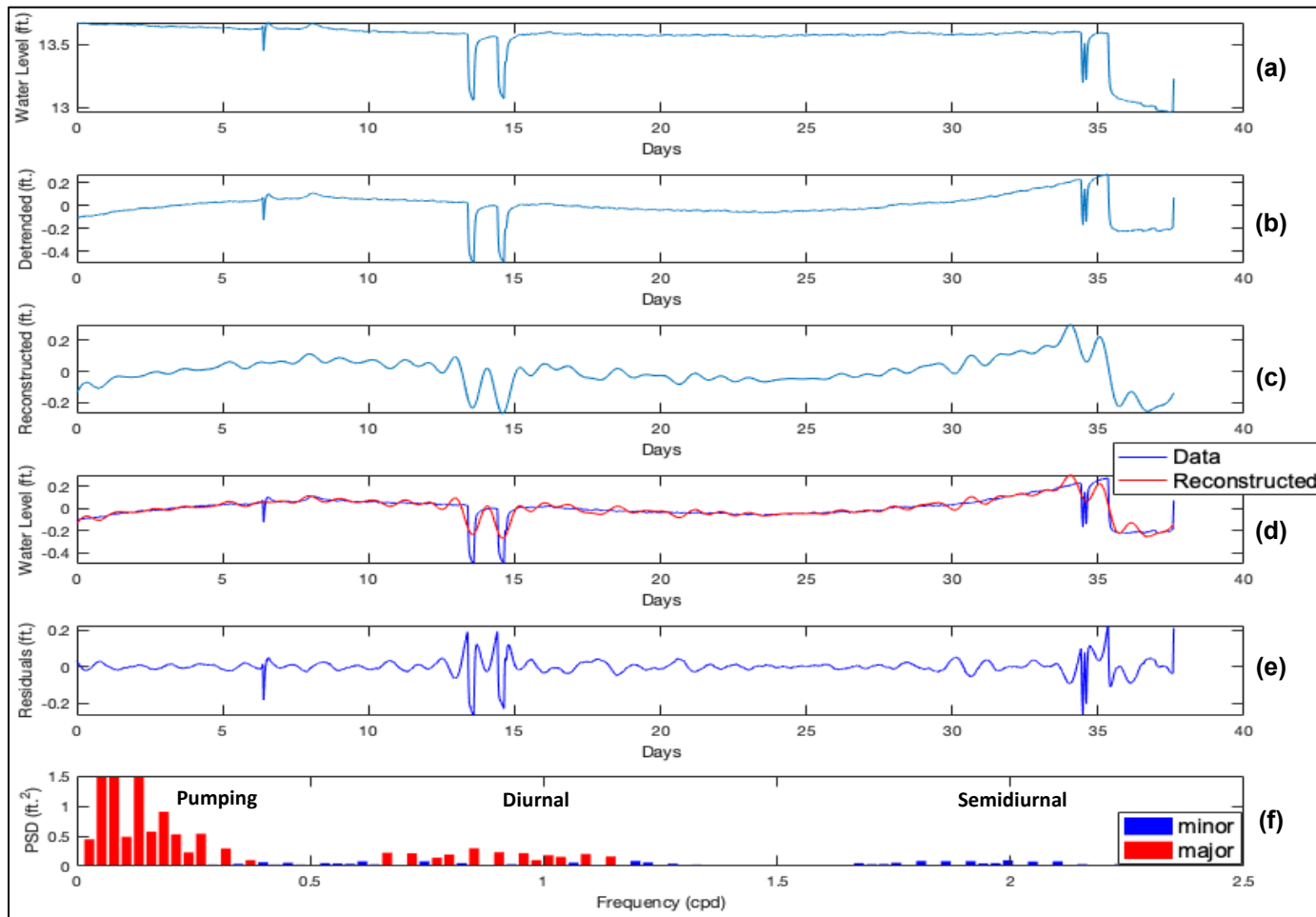


Figure 4.7 Spectral analysis of ABD-MW for 2023 Dry Season from April 26 to June 2. Respectively, a) raw data, b) raw data detrended, c) reconstructed data with cubic polynomial fit, d) reconstructed and detrended data, e) residuals represented as difference between reconstructed and detrended data, and f) power spectra with frequencies with major and minor signals identified.

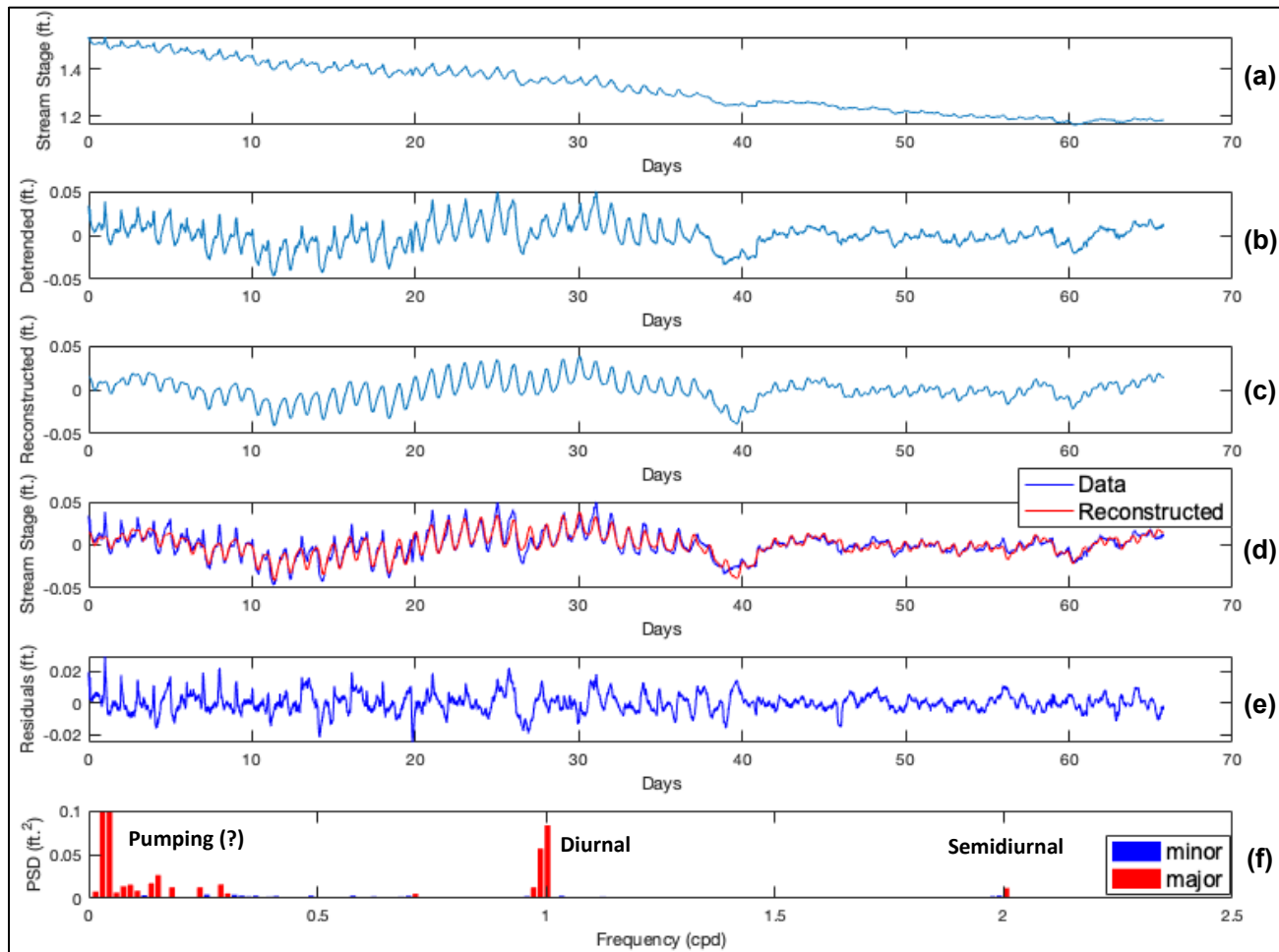


Figure 4.8 Spectral analysis of LO-P1 for 2023 Dry Season from June 9 to August 14. Respectively, a) raw data, b) raw data detrended, c) reconstructed data with cubic polynomial fit, d) reconstructed and detrended data, e) residuals represented as difference between reconstructed and detrended data, and f) power spectra with frequencies with major and minor signals identified.

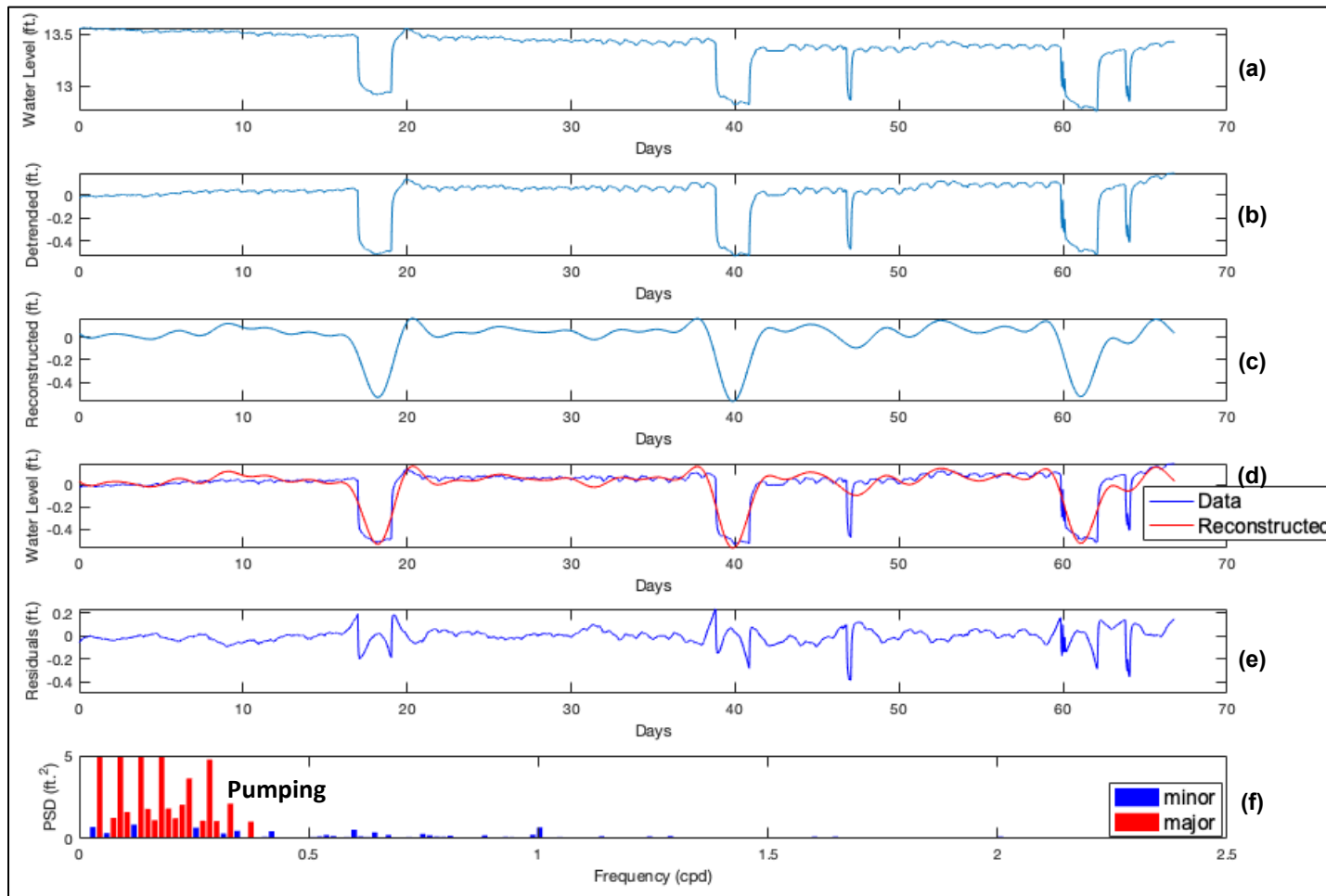


Figure 4.9 Spectral analysis of ABD-MW for 2023 Dry Season from June 9 to August 14. Respectively, a) raw data, b) raw data detrended, c) reconstructed data with cubic polynomial fit, d) reconstructed and detrended data, e) residuals represented as difference between reconstructed and detrended data, and f) power spectra with frequencies with major and minor signals identified.

4.1.3 Time Series Analysis of Stream Stage and Aquifer Water Levels at the Field 25 Site

Field 25 was irrigated approximately five times per week at various pumping rates, as detected by the amount of drawdown observed in F25-PW. Longer duration pumping events typically occurred either Thursday or Friday of a given week. The stream stage observed in F25-P1 exhibited strong diurnal fluctuations with no observable drawdown due to pumping from late April to mid-July as confirmed by the major signal at 1.0 cpd in Figure 4.12. Stream stage trended downward due to the drier weather and lack of precipitation as the 2023 Dry Season progressed resulting in the drying of the stream at the F25-P1 site on 7/22/2023. Figure 4.10 is an image of Stenner Creek at F25-P1 location on 8/11/2023 showing the dry streambed. The minor diurnal fluctuations observed in Figure 4.11 after 7/22/2023 was due to water being trapped within the F25-P1 piezometer.



Figure 4.10 Dry Stenner Creek at F25-P1 stream stage monitoring location on 8/11/2023.

Pumping induced drawdown observed in F25-PW appeared to induce drawdown within the stream stage data collected in F25-P1 from 7/15/2023 to 7/21/2023 (Figure 4.11). This is exhibited by the decline in stream stage once pumping was initiated followed by rapid recovery in F25-P1 with greater fluctuations in stream stage observed each consecutive day from 7/15/2023

to 7/21/2023. Larger pumping events occurred on 7/15/2023 and 7/17/2023 followed by shorter duration pumping events from 7/17/2023 to 7/19/2023 which induced 1.51-ft. of stream stage drawdown within F25-P1. This caused the first stream stage recovery point in the stream being observed 52.2 hours after initial drawdown. The stream ran dry shortly after the 7/21/2023 data collection which can be attributed to aquifer pumping and increasing temperatures in the later summer months.

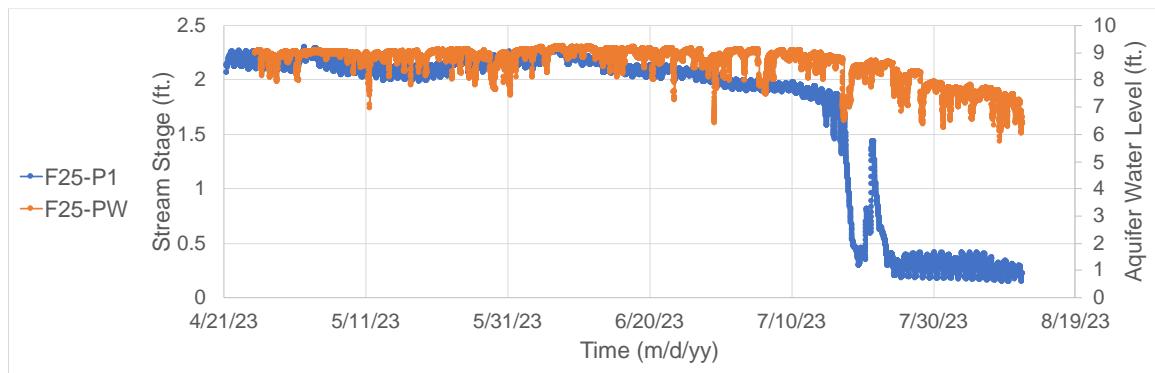


Figure 4.11 Stenner Creek stream stage and aquifer water level at Field 25 site during 2023 Dry Season.

4.1.4 Spectral Analysis of Stream Stage and Aquifer Water Levels at the Field 25 Site

The results of the spectral analysis for F25-P1 and F25-PW, presented in Figure 4.12 and Figure 4.13, respectively, show a strong diurnal signal at 1.0 cpd due to Et. F25-PW also shows a second major signal just below 1.0 cpd which is due to aquifer pumping considering the pumping well in Field 25 was used daily for irrigation. F25-P1 contained a strong diurnal signal; however, this diurnal signal was relatively weak compared to the signals detected at frequencies of 0.10 cpd and below. These stronger signals 0.10 cpd and below indicate larger pumping events, which occurred weekly or biweekly according to aquifer water level data collected in F25-PW, had a stronger impact on the F25-P1 data than what was visually determined in the time series analysis. The semidiurnal signal found within F25-P1 and F25-PW for the 2023 Dry Season was

relatively weak and classified as a minor signal. The PSD threshold for major components was $\text{PSD} > 1.0 \text{ ft.}^2$ and $\text{PSD} > 5.0 \text{ ft.}^2$ for F25-P1 and F25-PW, respectively.

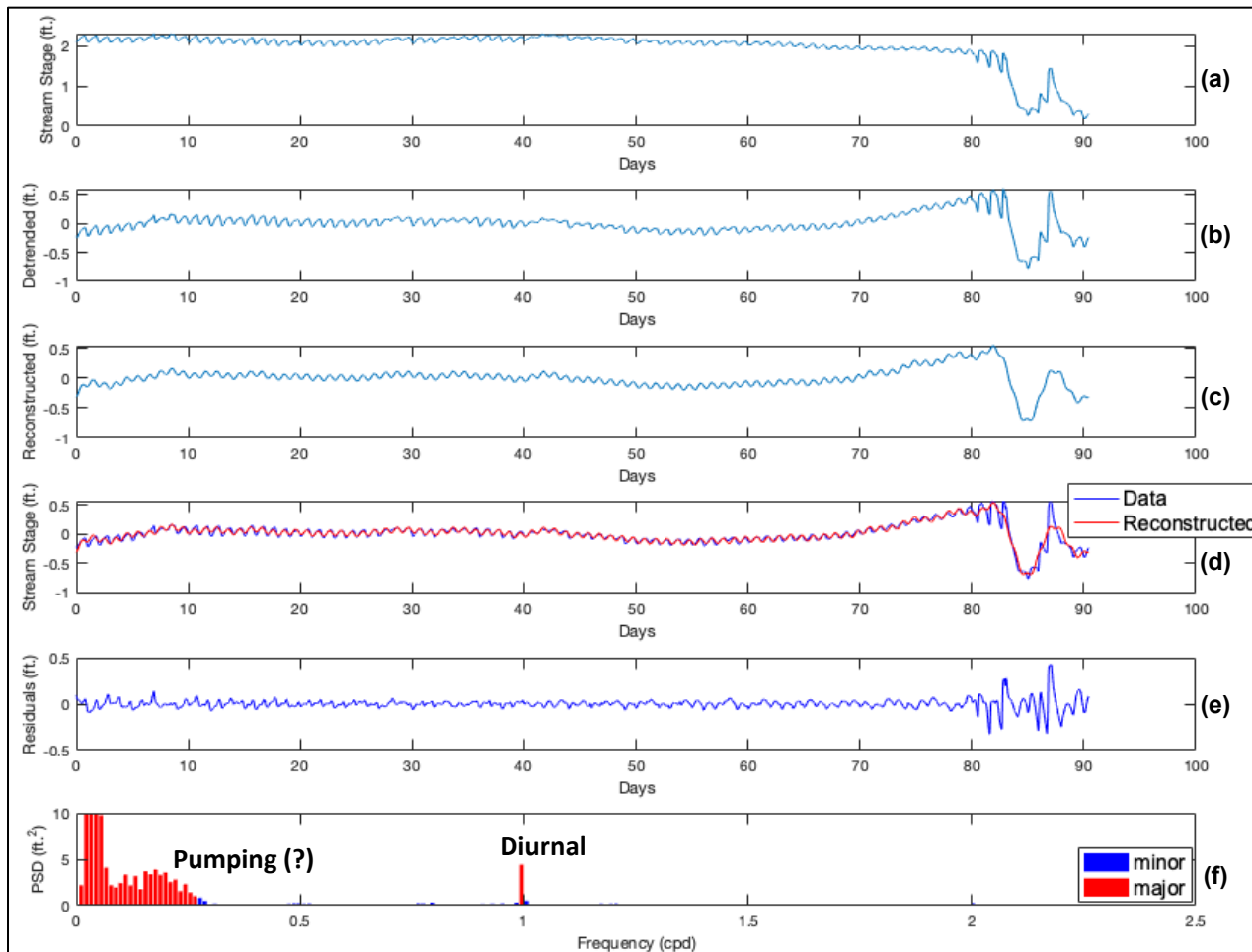


Figure 4.12 Spectral analysis of F25-P1 for 2023 Dry Season. Respectively, a) raw data, b) raw data detrended, c) reconstructed data with cubic polynomial fit, d) reconstructed and detrended data, e) residuals represented as difference between reconstructed and detrended data, and f) power spectra with frequencies with major and minor signals identified.

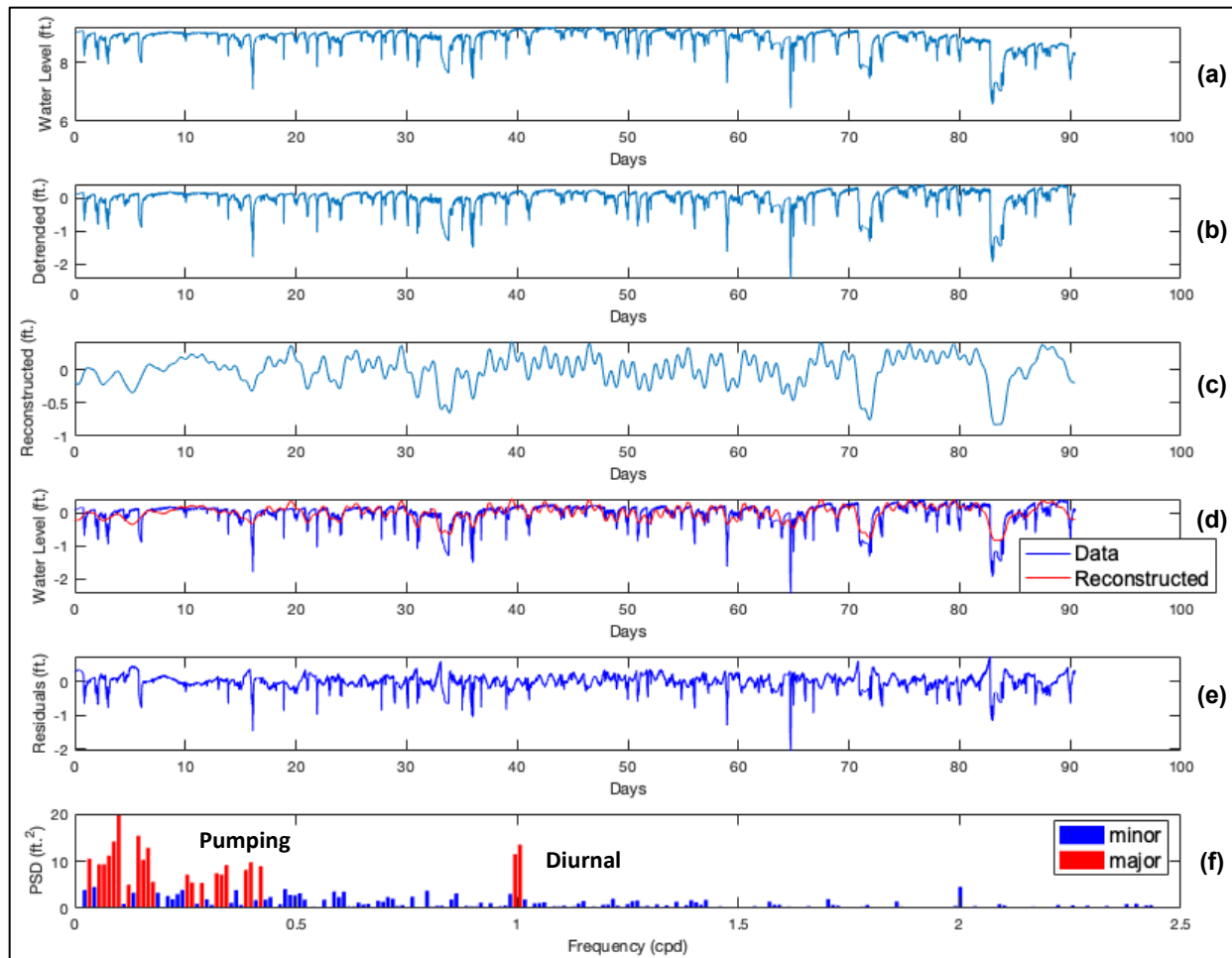


Figure 4.13 Spectral analysis of F25-PW for 2023 Dry Season. Respectively, a) raw data, b) raw data detrended, c) reconstructed data with cubic polynomial fit, d) reconstructed and detrended data, e) residuals represented as difference between reconstructed and detrended data, and f) power spectra with frequencies with major and minor signals identified.

4.2 Stream Discharge Response to Aquifer Pumping

The stream discharge recorded in Stenner Creek at the Lemon Orchard location displayed a general downward trend over the duration of the 2023 data collection period associated with the drying of the aquifer-stream system as the dry season progresses. The highest recorded discharge rate was the first recording on 6/14/2023 which measured 2.12 cfs of discharge. The lowest recorded discharge rate was measured to be 0.84 cfs during the pumping event on 8/8/2023. The approximated depletion quantities derived when longer term pumping was observed in the ABD-MW, are 0.23 cfs, 0.27 cfs, and 0.23 cfs during the pumping events 6/26/2023 to 6/28/2023, 7/18/2023 to 7/20/2023, and 8/7/2023 to 8/9/2023, respectively. This was calculated by taking the discharge rate recorded prior to the commencement of aquifer pumping and subtracted by the lowest discharge rate recorded during aquifer pumping. The dips in discharge rate corresponded to both shorter and longer duration pumping events indicating aquifer pumping had a strong impact on the measured stream discharge rates.

The stream discharge rates measured appeared to have a correlation with aquifer pumping induced drawdown observed within ABD-MW. Sudden declines in the stream discharge rate were observed seven times, five of which correspond to five observed pumping events. Two of the drops in the discharge rate were observed on 7/12/2023 and 8/1/2023 when pumping was not detected in ABD-MW. However, these drops that do not correspond to pumping in LO-PW could be attributed to upstream pumping. Each drop in stream discharge rates during pumping, observed by the sudden drop in aquifer water levels recorded in ABD-MW, recovered to, or exceeded discharge rates prior to the subject pumping event. The largest discharge rate recovery post-pumping occurred from 6/27 to 6/29 which also corresponds to the largest aquifer water level recovery observed within the ABD-MW implying surface and subsurface discharge are hydraulically connected.

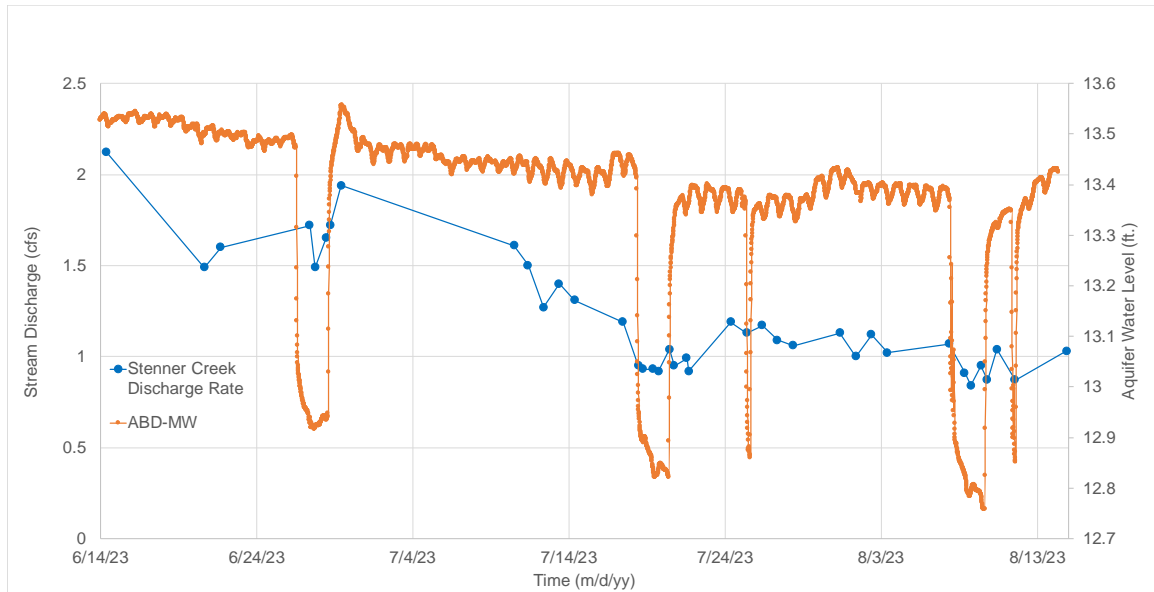


Figure 4.14 Stream discharge in Stenner Creek and aquifer water level in ABD-MW at Lemon Orchard site during 2023 Dry Season.

Only four discharge rates measurements were collected at the Field 25 location before the stream ran dry. Considering the pumping well used to irrigate Field 25 was used daily, discharge rates were not recorded as continuously as the Lemon Orchard site but were instead recorded the day before, during, and after the largest pumping events occurred due to accessibility issues at the F25-P1 site. This method resulted in only four discharge rates being recorded prior to the stream running dry at the Field 25 location. The discharge rates recorded prior to the stream running dry for Field 25 are presented in Table 4.4 below. The discharge rate reduced from a maximum of 0.57 cfs recorded on 6/22/2023, to a minimum of 0.00 cfs, observed on 7/17/2023 when the stream ran dry at the discharge measuring location. A pool of water remained at F25-P1 despite the stream running dry at the discharge collecting location. The rapid decline of stream discharge at the Field 25 location over the three-day span from 7/14 to 7/17 corresponds to the increased fluctuations in observed in stream stage at F25-P1 from 7/15/2023 onwards depicted in Figure 4.11. The Field 25 reach had disconnected pools of water with no visible discharge at multiple locations. The implications of no recordable discharge rate on drawdown observed in the stream due to aquifer pumping is discussed in more detail in the Discussion chapter.

Table 4.4 Stenner Creek discharge rates recorded at the Field 25 site.

Field 25 Discharge Rates		
Date	Time	Discharge Rate (cfs)
6/22/23	10:07 AM	0.57
7/14/23	8:43 AM	0.15
7/14/23	5:52 PM	0.01
7/15/23	8:21 AM	0.08
7/17/23	9:06 AM	0.00

4.3 Streambed Hydraulic Conductivity

The measured streambed hydraulic conductivity (K) in Stenner Creek is relatively high when classifying the calculated K into the typical ranges of K values below in Table 4.5 (Domenico & Schwartz, 1990). Table 4.5 provides a range of values for each type of water bearing materials with the most conductive material being gravels and coarse sand and the least conductive material being till and various forms of clay.

Table 4.5 Typical hydraulic conductivity values of water bearing materials.

Material	Hydraulic Conductivity (fps)	
	Min	Max
Gravel	9.84×10^{-4}	9.84×10^{-2}
Coarse Sand	2.95×10^{-6}	1.97×10^{-2}
Medium Sand	2.95×10^{-6}	1.64×10^{-3}
Fine Sand	6.56×10^{-7}	6.56×10^{-4}
Silt, Loess	3.28×10^{-9}	6.56×10^{-5}
Till	3.28×10^{-12}	6.56×10^{-6}
Clay	3.28×10^{-10}	1.54×10^{-8}
Unweathered marine clay	2.62×10^{-12}	6.56×10^{-9}

There were certain segments of Stenner Creek that did not yield successful pneumatic slug tests due to the presence of high concentrations of gravel and solid rock which were impenetrable and thus made well installation infeasible. Additionally, segments of the Stenner Creek streambed with high amounts of gravel that well installation was successful often did not yield meaningful

data due to the water level within the well recovering too quickly for the transducer to record an adequate number of measurements. All tests that did not yield successful results are noted with a value of "X" in their respective cells. Lastly, as depicted in the images below in Figure 4.15 and Figure 4.16, high amounts of Chlorophyta, or green algae, were present within the stream at all locations. The presence of the Chlorophyta did not impede well installations, nor the results of the pneumatic slug tests performed.

4.3.1 Lemon Orchard Reach Pneumatic Slug Test Results

The pneumatic slug tests performed in the Lemon Orchard reach of Stenner Creek only yielded 19 successful tests out of 54 slug tests attempted. Figure 4.15 provides a sequence of images taken within the Lemon Orchard reach providing a visual representation of the streambed material and surrounding area. As depicted in the images below, there is a high concentration of gravel and stones within the streambed at all locations which made it difficult to obtain successful slug test data given the high porosity of the streambed material and the limitations of the transducer's recording capabilities. The 300-ft. zone upstream of LO-P1 was the only upstream zone that yielded successful results. The tests performed at the midpoint of the upstream reach and in the direct vicinity of LO-P1 did not yield successful results because of the high concentrations of gravel and impermeable rock which did not allow for well installation or yielded inadequate data for accurate calculations of K. The results from the pneumatic slug tests performed in the lemon orchard reach are found in Table 4.6.

The location approximately 300-ft. upstream of the LO-P1 location had a mixture of sandy soils and gravel upon visual examination the wetted streambed with high concentrations of gravel along the dry banks. The highest K value was calculated in Test 3 of the left bank which could be due to recording error considering it deviates from the previous two tests at that location. However, since the deviated calculation is still in the range of probable values for gravel material and the sediment appears to be gravel upon visual examination, this is negligible. The values that

were recorded for this zone ranged from 9.01×10^{-4} feet per second (fps) to 2.42×10^{-3} fps which are within the range of gravel material, as stated in Table 4.5.

Directly downstream of the LO-P1 location was observed to be predominantly gravel mixed with loose silty soils upon visual examination. The loose soil allowed for the well to be installed in the streambed at this location which yielded successful results for all slug tests conducted in this zone. The K values calculated for this zone range from 2.78×10^{-3} fps to 3.26×10^{-3} fps indicating the material is gravel or coarse sand which agrees with the visual observations. Therefore, although this zone is still highly conductive and has a high potential for storage within the streambed, it is relatively low compared to the segments that have higher concentrations of highly porous gravel.

The streambed downstream from LO-P1 progressively contains higher concentrations of gravel making it more difficult to collect adequate data for K calculations. The midpoint of the downstream segment only yielded two successful tests and the furthest downstream zone tested in this reach produced four successful tests out of nine attempted. The values in these two zones range from 1.35×10^{-3} fps to 4.39×10^{-3} fps indicating this segment is gravel material and therefore has high storage potential.



Figure 4.15 Stenner Creek slug test location images at the Lemon Orchard reach.

Table 4.6 Pneumatic slug test results at the Lemon Orchard reach.

Segment	Zone	Hydraulic Conductivity (fps)		
Upstream	300 ft.	Test 1	Test 2	Test 3
	Right	X	X	X
	Middle	2.42x10 ⁻³	X	X
	Left	9.01x10 ⁻⁴	9.10x10 ⁻⁴	1.08x10 ⁻³
	150 ft.			
	Right	X	X	X
	Middle	X	X	X
	Left	X	X	X
	6 ft.			
	Right	X	X	X
	Middle	X	X	X
	Left	X	X	X

Downstream	6 ft.	Test 1	Test 2	Test 3
	Right	1.52x10 ⁻³	1.91x10 ⁻³	2.04x10 ⁻³
	Middle	2.64x10 ⁻³	2.07x10 ⁻³	1.57x10 ⁻³
	Left	4.50x10 ⁻⁴	5.06x10 ⁻⁴	6.12x10 ⁻⁴
	150 ft.			
	Right	X	X	X
	Middle	3.26x10 ⁻³	2.78x10 ⁻³	X
	Left	X	X	X
	300 ft.			
	Right	1.35x10 ⁻³	3.42x10 ⁻³	X
	Middle	4.39x10 ⁻³	X	4.28x10 ⁻³
	Left	X	X	X

4.3.2 Field 25 Reach Pneumatic Slug Test Results

The pneumatic slug test performed in the Field 25 reach of Stenner Creek yielded 28 successful tests out of 54 slug tests attempted. Figure 4.16 provides a sequence of images taken within the Field 25 reach providing a visual representation of the streambed material and surrounding area. As depicted in the images below, there is a high concentration of gravel and stones within the streambed at all locations, however, there were pockets of the streambed which had higher concentrations of sands and clayey material which allowed for successful well installations and slug tests. Table 4.7 shows the slug test results and calculated K values for the Field 25 reach.

The 300-ft. zone downstream of F25-P1 was the only zone that did not yield a successful test due to the high concentrations of gravel that were impenetrable with the available equipment. The highest success rate occurred within the 300-ft. zone upstream of F25-P1 which had higher concentrations of sands and clayey material allowing for well installation. The midpoint and closest zones upstream of F25-P1 also provided more successful tests compared to the downstream testing locations. The concentration of impermeable gravel progressively increased moving downstream from the F25-P1 location.

The 300-ft. upstream zone of the LO-P1 location was observed to have a mixture of sandy and clayey soils with lower concentrations of gravel upon visual examination of the wetted streambed with high concentrations of gravel and stones along the dry banks. The highest K value was calculated in Test 2 in the middle of the streambed and the lowest recorded in Test 1 along the right side of the streambed. The recorded values for this zone ranged from 7.30×10^{-4} fps to 3.72×10^{-3} which are within the range of gravel material, as stated in Table 4.5. The 150-ft. zone upstream of F25-P1 provided tests that ranged from 6.41×10^{-4} fps to 2.66×10^{-3} fps. The 6-ft. zone upstream of F25-P1 yielded greater K values than the 300-ft. and 150-ft. zones which coincides with the visual analysis of higher concentrations of gravel and more conductive materials in the streambed moving downstream from the top to the bottom of the Field 25 reach. The highest K measurement, 2.96×10^{-2} fps, was recorded in the 6-ft. upstream zone. Higher K values could be recorded in the areas with higher concentrations of gravel with the appropriate equipment.

The downstream segment of the Field 25 reach was observed to be predominantly gravel with some pockets of lower diameter gravel and sand which were penetrable with the available well development materials. The areas with looser sediment allowed for the well to be installed in the streambed at the 6-ft. and 150-ft. downstream locations which yielded successful tests. The K values calculated for the 6-ft. zone range from 4.44×10^{-4} to 1.59×10^{-3} indicating the material is gravel which agrees with the visual observations. The values calculated for the 150-ft. zone range

from 1.70×10^{-4} to 2.03×10^{-3} indicating the material is gravel or coarse sand which also agrees with the visual observations. The 300-ft. zone was comprised of impenetrable gravel and therefore did not yield any successful tests.



Figure 4.16 Stenner Creek slug test location images at the Field 25 reach.

Table 4.7 Pneumatic slug test results at the Field 25 reach.

Segment	Zone	Hydraulic Conductivity (fps)		
Upstream	300 ft.	Test 1	Test 2	Test 3
	Right	7.30×10^{-4}	8.86×10^{-4}	1.29×10^{-3}
	Middle	2.78×10^{-3}	3.72×10^{-3}	3.08×10^{-3}
	Left	1.06×10^{-3}	1.31×10^{-3}	1.47×10^{-3}
	150 ft.			
	Right	6.41×10^{-4}	9.17×10^{-4}	1.22×10^{-3}
	Middle	X	2.66×10^{-3}	X
	Left	X	X	2.32×10^{-3}
	6 ft.			
	Right	X	X	3.52×10^{-3}
	Middle	2.96×10^{-2}	X	X
	Left	1.15×10^{-3}	1.74×10^{-3}	1.22×10^{-3}

Downstream	6 ft.	Test 1	Test 2	Test 3
	Right	4.44×10^{-4}	7.57×10^{-4}	1.31×10^{-3}
	Middle	X	X	X
	Left	1.39×10^{-3}	1.59×10^{-3}	1.36×10^{-3}
	150 ft.			
	Right	X	X	X
	Middle	X	X	2.03×10^{-3}
	Left	X	1.70×10^{-3}	1.94×10^{-3}
	300 ft.			
	Right	X	X	X
	Middle	X	X	X
	Left	X	X	X

CHAPTER 5: DISCUSSION

5.1. Stream Stage Response to Aquifer Pumping

The stream stage data collected during the 2022 Dry Season at the Lemon Orchard site displayed observable drawdown responses to aquifer pumping which corresponded to drawdown observed within the ABD-MW, as shown above in Figure 4.2. The spectral analysis performed on the 2022 Dry Season Pumping Events for both LO-P1 and ABD-MW, Figure 4.4 and Figure 4.5, respectively, validate this determination. Both Figure 4.4 and Figure 4.5 showed the strongest signals at 0.10 cpd and below which corresponds to the bi-weekly pumping events within LO-PW, which is similar to the findings within the spectral analysis presented in Malama et al. (2021). LO-P1 did not display any major diurnal (1 cpd) nor semidiurnal (2 cpd) signals which is likely due to the lower discharge rates during the later summer and fall months of 2022 and overwhelming influence of aquifer pumping on the collected stream stage data. Diurnal fluctuations in stream stage spectral analyses are attributable to ET (Malama et al., 2021) and the semidiurnal fluctuations are attributable to ocean and earth tides (Bredehoeft, 1967; Hsieh et al., 1988; Rojstaczer & Riley, 1990; MacAllister et al., 2016).

Conversely, the data gathered in LO-P1 for the 2023 Dry Season did not show significant drawdown due to aquifer pumping events with some minor drawdown events later in the 2023 Dry Season, as shown in Figure 4.3. Kollet & Zlotnik (2003) found that stream stage drawdown can be ignored in groundwater modeling since the stream discharge rate is two orders higher than the aquifer pumping rate. However, this implies that stream stage drawdown is relevant at lower degrees of stream discharge. This is confirmed during the 2022 Dry Season stream stage and aquifer water level time series and spectral analyses for the data gathered from LO-P1 and ABD-MW, respectively, as stream stage displayed observable drawdown when stream discharge was low.

Although stream stage drawdown was not observable in the 2023 Dry Season time series analysis, the spectral analysis performed for the first and second portion of 2023 Dry Season in LO-P1 and F25-P1 displayed major signals at 0.1 cpd and below which corresponds to the frequency of major aquifer pumping events. Diurnal and semidiurnal signals were also identified as major signals in all stream stage measuring locations, as shown in Figure 4.6, Figure 4.8, and Figure 4.13, respectively. The diurnal signal in LO-P1 was stronger in the first portion (4/26/2023 to 6/2/2023) relative to the second portion (6/9/2023 to 8/14/2023) of the 2023 Dry Season which is expected based on the findings in Lundquist & Cayan, (2002) and Condon & Maxwell, (2019) who found that higher discharge rates correspond to stronger diurnal signals and weaker pumping induced signals. The 2023 Dry Season corresponds to higher discharge rates earlier in season and lower discharge rates as the Dry Season progresses. Considering the strengthening of the diurnal signal as the Dry Season progresses, these findings agree with the conclusions of Lundquist & Cayan (2002) and Condon & Maxwell (2019) which determined that lower discharge rates diminish ET signals. However, the 2022 Dry Season spectral analysis (Figure 4.4), when discharge was nonexistent and aquifer pumping was at its highest, did not detect any major diurnal signal which disagrees with the findings of Condon & Maxwell (2019). This is likely due to the overwhelming impact that aquifer pumping had on the collected stream stage and aquifer water level data within LO-P1 and ABD-MW.

This findings in this study support the findings of Kollet & Zlotnik (2003) who found that stream stage drawdown can be ignored in groundwater modeling when stream discharge is measurable implying that stream stage drawdown should be accounted for when discharge is low. Stream stage drawdown was observable when stream discharge was low during the 2022 Dry Season at the Lemon Orchard site and the latter half of the 2023 Dry Season at the Field 25 site. Therefore, the first hypothesis (H1) "Pumping from an aquifer will reduce stream stage in a connected stream" is confirmed under the condition that surface water discharge must be low or nonexistent for observable stream stage drawdown in response to aquifer pumping to be observable.

5.2. Stream Discharge Response to Aquifer Pumping

Discharge rates recorded in Stenner Creek from 6/14/2023 to 8/14/2023 at the Lemon Orchard site exhibited a general downward trend over the course of the 2023 Dry Season with sudden drops in the discharge rate occurring when pumping was detected in the ABD-MW, as exhibited in Figure 4.14. These sudden drops in the discharge rate were followed by recovery of the stream discharge rate once pumping was completed with varying degrees of recovery based on the availability of subsurface flows. This agrees with the findings of previous research (Lapides et al., 2022; Barlow & Leake, 2012; Hunt, 1999, 2003, 2014; Theis, 1941, and others) which determined that pumping from an aquifer which is hydraulically connected to a stream will induce stream depletion.

The negligible discharge rate observed at the Lemon Orchard site during the 2022 Dry Season corresponds to the visible drawdown observed within the stream stage from the time series analysis. The higher discharge rates associated with the 2023 Dry Season corresponded to no visible drawdown of stream stage at LO-P1 in the early phase of the 2023 Dry Season with drawdown becoming more observable during the latter portion of the 2023 Dry Season as discharge rates declined which is consistent with the findings in Kollet & Zlotnik (2003). Only four stream discharge measurements were taken at the Field 25 site prior to the stream running dry on 7/17/2023. However, the observed stream stage in F25-P1 appeared to exhibit drawdown characteristics in response to pumping events like the findings in the LO-P1 2022 Dry Season time series analysis. This indicates that there is a hydraulic connection within the aquifer-stream system between the measured stream discharge rate and observed stream stage drawdown within a stream due to aquifer pumping (Lapides et al., 2022; Barlow & Leake, 2012; Hunt, 1999, 2003, 2014; Theis, 1941, and others).

Comparing the results of the stream stage and stream discharge measurements indicates that the constant head boundary assumption or treating streams as a constant supply of water (Dirichlet), is invalid during lower discharge rates but is valid during higher stream discharge rates within Stenner Creek at the Lemon Orchard pumping site which agrees with the conclusions of (Kollet & Zlotnik, 2003). Therefore, the second hypothesis (H2) can be confirmed that pumping within an aquifer will result in stream depletion. However, this determination unique to the data collected in this study which is influenced by the hydrogeologic composition of the aquifer-stream system and the pumping rates within each pumping well.

5.3. Streambed Hydraulic Conductivity

The results from the pneumatic slug tests performed in the streambed of Stenner Creek at the Field 25 and Lemon Orchard sites suggest that the streambed storage is relatively high. The findings in Huang et al. (2020) determined that streambed storage is highly influential in groundwater modeling and the observed stream stage drawdown. This is exhibited in this study when observing the stream stage drawdown duration in LO-P1 compared to ABD-MW during the 2022 Dry Season where the stream was found to recover slower compared to the aquifer implying that the stream has a high amount of storage potential. All successful tests conducted indicate that the material within the streambed is highly conductive gravels and coarse sands. Only 49 out of the 108 tests performed resulted in successful streambed K measurements, however, the areas where tests were unsuccessful were likely to be the most conductive areas because of the high concentrations of gravel. Gravel is the most conductive water bearing material (Domenico & Schwartz, 1990) and was also responsible for unsuccessful tests, whether it be the impermeability and inability to install the well or the rapid recovery of the water column within the well due to the high K of the surrounding material. Refer to the Limitations section in the Methodology chapter for more information on why many tests were unsuccessful. Therefore, the trials that were unsuccessful, denoted with an “X” in Table 4.6 and Table 4.7, would likely be

the most hydraulically conductive portions of the streambed within each respective reach of Stenner Creek.

Since the calculated K for each trial are within the gravel and coarse sands material K ranges (Domenico & Schwartz, 1990), it is inconclusive if the various responses in stream stage and stream discharge observed at the Lemon Orchard and Field 25 sites were impacted by the streambed hydraulic conductivity. Additionally, considering the stream ran dry at Field 25 where the discharge measurements were recorded previously, we were not able to compare the stream discharge and stage data gathered at each reach to validate this claim. The higher K values within the Field 25 reach could be a contributor to the stream running dry along this reach during the study period (Lackey et al., 2015; Neupauer et al., 2020); however, this is more likely due to more frequent aquifer pumping from F25-PW which reduces the recovery of the water levels within the stream and subsurface aquifer (Zipper et al., 2022). The Lemon Orchard site also exhibited high K values within the streambed, however the stream continued to flow throughout the 2023 summer. This is likely due to the Lemon Orchard site being hydraulically down gradient from the Field 25 site and therefore receives higher quantities of surface and subsurface discharge. The impacts of streambed hydraulic conductivity on stream depletion and drawdown have been modeled and studied extensively by various researchers all of which conclude that higher streambed K will result in greater stream depletion (Huang et al., 2020; Lackey et al., 2015; Neupauer et al., 2020; Wang et al., 2016; Zipper et al., 2022, and others).

Lackey et al. (2015) modeled the sensitivity of stream depletion to streambed hydraulic conductivity and geometry of the streambed itself, both of which are inputs to streambed conductance, which concluded that more hydraulically conductive streambeds are expected to result in higher stream depletion rates if pumping occurs in a hydraulically connected aquifer. The findings in this study agree with the modeled findings in Lackey et al. (2015) as the K within the streambed was found to be in the most conductive range of potential water transmitting materials

at all testing locations and stream discharge was observed to decrease during aquifer pumping, and recover once pumping concluded. This study did not quantify the amount of stream depletion relative to various hydraulically conductive materials found within the streambed but did identify a relationship between aquifer pumping and observed stream depletion. Therefore, the third hypothesis (H3) that “higher degrees of change in stream stage and discharge will occur in segments of the stream that are more hydraulically conductive” is inconclusive since the streambed hydraulic conductivity was within the same range of highly conductive gravels and coarse sands at all tested locations.

5.4. Future Considerations

Future research should consider the following to further address the stream depletion paradox. It is advised to conduct a multi-year study where stream stage, aquifer water levels, and stream discharge are collected continuously. Although this study was able to compare two dry season periods, it would be beneficial to continue data collection into the fall months up to the first rain event of the wet season to determine the impacts of the lowest quantity of stream discharge each year on the observable drawdown in stream stage during aquifer pumping. This study was limited to the pumping schedule controlled by the Cal Poly Agricultural Department to irrigate the Lemon Orchard and Field 25. It would be beneficial to control the pumping duration and pumping rate to introduce more controlled variables to be able to relate the observed stream stage drawdown and stream depletion based on the pumping rate within the subject pumping well.

It is also advised that the stream discharge data collection be conducted from the final precipitation event of a wet season to the first precipitation of the following wet season to better understand the variability and sensitivity of stream discharge across the entire dry season and under various pumping conditions. This would allow researchers to better determine at which discharge rate threshold does observable stream depletion occur and how stream depletion due to pumping varies across the entire dry season.

Lastly, it is advised that streambed hydraulic conductivity in-situ measurements be recorded using a transmitter and data logger to collect more data points over the same testing duration and thus improve the AQTESOLV streambed hydraulic conductivity estimates. A transmitter can collect data points every decisecond whereas the transducer used for this study can only collect a data point every second. This means a transmitter can collect ten times the amount of data points compared to the transducer over the same slug test duration. Obtaining high quantities of data points during the water level recovery phase within the slug test well would provide a better estimate of K using AQTESOLV. Additionally, the streambed hydraulic conductivity measurements collected have inherent biases due to the limitations of the well and insertion equipment used in this study. The well was only able to be installed in certain portions of the streambed due to impenetrability of the streambed with the PVC well. Utilizing stronger materials for the well casing which can be inserted into the streambed with a more forceful method would allow for streambed hydraulic conductivity values to be collected at the areas with higher gravel concentrations.

Rus et al., (2001) concluded that there could be high variability in materials within a streambed which could alter the connectivity of the stream and thus impact the stream depletion rate. This study only inserted wells approximately 10-in. into the streambed subsurface which was found to be highly conductive material. The heterogeneity in streambed materials and associated conductance within Stenner Creek at greater depths could better explain the observed stream depletion rates. However, as found in Lackey et al. (2015), the streambed conductance can be assumed to be a homogenous value throughout the subject stream if a certain threshold of aquifer hydraulic conductivity and streambed conductance values are met. This study did not delve into the streambed K heterogeneity and its impacts on the observed stream discharge rates.

CHAPTER 6: CONCLUSION

The use of a constant head (Dirichlet) boundary condition within groundwater modeling assumes stream stage is fixed and does not experience any drawdown in the event of pumping from an interconnected aquifer despite the presence of stream depletion. Stream stage remaining fixed during aquifer pumping implies that streams and lakes in a groundwater model act as an infinite supply of water. This paradox of stream depletion occurring without stream stage drawdown is referred to as the stream depletion paradox in Malama et al. (2022). This study aimed to determine if the stream depletion paradox is realized when pumping occurs within an aquifer-stream system by measuring stream stage, aquifer water levels, stream discharge, and the hydraulic conductivity of the subject streambed.

This study site is Stenner Creek, a tributary to the San Luis Obispo Creek, and the agricultural fields, namely the Lemon Orchard and Field 25, located on the California Polytechnic University, San Luis Obispo campus. The first portion of this study passively collected stream stage and aquifer water level data and analyzed through time series and spectral analyses to determine if there is any observable drawdown within the stream when aquifer pumping occurs. The results from this portion of the study conditionally confirmed the first hypothesis (H1) that stream stage drawdown was observed when aquifer pumping occurred under the condition that stream discharge was low or nonexistent. Stream stage did not display the same observable drawdown when stream discharge rates were high in the spring and early summer months. The second portion of this study actively collected stream discharge measurements before, during, and after aquifer pumping to determine if stream depletion occurred within the subject aquifer-stream system under aquifer pumping conditions. The results of this portion confirm the findings of previous studies that aquifer pumping from an interconnected aquifer-stream system would result in stream depletion. Stream depletion occurred during aquifer pumping during all measured aquifer pumping events, which confirms the second hypothesis (H2) that stream depletion would occur during aquifer pumping. The final portion of this study conducted pneumatic slug tests

within the streambed of Stenner Creek to collect in-situ streambed hydraulic conductivity measurements. The results indicate that the streambed of the Lemon Orchard and Field 25 reaches consist of highly conductive material, namely gravels and coarse sands and, therefore, the streambed has high storage capacity at both locations. Considering the streambed material was within the same ranges at both the Lemon Orchard and Field 25 reaches, the third hypothesis (H3) was inconclusive.

Future advancements in addressing the stream depletion paradox are required to better refine groundwater modeling inputs and sustainably manage aquifer-stream systems. Sustainable management of aquifers, as mandated under SGMA, will require accurate groundwater modeling to create effective groundwater sustainability and management plans which will have enduring impacts on our environment, society, and economy. This research, subsequent data collection, and improvements to groundwater modeling will allow water managers and planners to sustainably manage local water systems which will be relied upon for generations to come.

REFERENCES

- Baalousha, H. M. (2012). Drawdown and stream depletion induced by a nearby pumping well. *Journal of Hydrology*, 466–467, 47–59. <https://doi.org/10.1016/j.jhydrol.2012.08.010>
- Barlow, P., Ahlfeld, D., & Dickerman, D. (2003). Conjunctive-Management Models for Sustained Yield of Stream-Aquifer Systems. *Journal of Water Resources Planning and Management-Asce - J WATER RESOUR PLAN MAN-ASCE*, 129. [https://doi.org/10.1061/\(ASCE\)0733-9496\(2003\)129:1\(35\)](https://doi.org/10.1061/(ASCE)0733-9496(2003)129:1(35))
- Barlow, P., & Leake, S. A. (2012, November 1). *Circular 1376: Streamflow Depletion by Wells—Understanding and Managing the Effects of Groundwater Pumping on Streamflow*. United States Geological Survey. <https://pubs.usgs.gov/circ/1376/>
- Baudic, G., Auger, A., Ramiro, V., & Lochin, E. (2021). 14—Using emulation to validate applications on opportunistic networks. In J. J. P. C. Rodrigues (Ed.), *Advances in Delay-Tolerant Networks (DTNs) (Second Edition)* (pp. 273–280). Woodhead Publishing. <https://doi.org/10.1016/B978-0-08-102793-6.00014-X>
- Berbel, J., & Esteban, E. (2019). Droughts as a catalyst for water policy change. Analysis of Spain, Australia (MDB), and California. *Global Environmental Change*, 58, 101969. <https://doi.org/10.1016/j.gloenvcha.2019.101969>
- Bredehoeft, J. D. (1967). Response of well-aquifer systems to Earth tides. *Journal of Geophysical Research (1896-1977)*, 72(12), 3075–3087. <https://doi.org/10.1029/JZ072i012p03075>
- Brodie, R. S., Sundaram, B., Tottenham, R., Hostetler, S., & Ransley, T. (2007). *An Overview of Tools for Assessing Groundwater-Surface Water Connectivity*. Australian Government - Department of Agriculture, Fisheries, and Forestry. chrome-extension://efaidnbmnnnibpcajpcglclefindmkaj/https://www.researchgate.net/profile/Baskaran-Sundaram/publication/266472444_An_Overview_of_Tools_for_Assessing_Groundwater-Surface_Water_Connectivity/links/55388abb0cf226723ab6306a/An-Overview-of-Tools-for-Assessing-Groundwater-Surface-Water-Connectivity.pdf

- Brunner, P., & Simmons, C. T. (2011). *HydroGeoSphere: A Fully Integrated, Physically Based Hydrological Model*. <https://doi.org/10.1111/j.1745-6584.2011.00882.x>
- Cal Poly Department of Agricultural Operations. (2004, September 27). *Well Drilling Logs Performed by Earth Systems Pacific* [Text]. College of Agriculture, Food and Environmental Sciences. <https://cafes.calpoly.edu/agops>
- California Department of Water Resources. (2023a, March 24). *Harnessing Series of Winter Storms, California Increases State Water Project Allocation*. <https://water.ca.gov/News/News-Releases/2023/March-23/Harnessing-Series-of-Winter-Storms-California-Increases-State-Water-Project-Allocation>
- California Department of Water Resources. (2023b, June 14). *Drought*. <https://water.ca.gov/Water-Basics/Drought>
- California Department of Water Resources. (2023c, June 27). *California Water Watch*. <https://cww.water.ca.gov/>
- California Department of Water Resources, D. (n.d.). *SGMA Basin Prioritization Dashboard*. Retrieved June 29, 2023, from <https://gis.water.ca.gov/app/bp-dashboard/final/>
- California Department of Water Resources, S. of. (2016, December 30). *Best Management Practices and Guidance Documents*. <https://water.ca.gov/Programs/Groundwater-Management/SGMA-Groundwater-Management/Best-Management-Practices-and-Guidance-Documents>
- California greatly increases State Water Project allocations*. (2023, March 29). WaterWorld. <https://www.waterworld.com/drinking-water/distribution/press-release/14291684/california-greatly-increases-state-water-project-allocations>
- Chan, Y. K. (1976). Improved image-well technique for aquifer analysis. *Journal of Hydrology*, 29, 149–164. [https://doi.org/10.1016/0022-1694\(76\)90011-1](https://doi.org/10.1016/0022-1694(76)90011-1)
- Chanson, H. (2004). *Numerical modelling of steady open channel flows: Backwater computations—ScienceDirect*. <https://www.sciencedirect.com/science/article/pii/B9780750659789500222>

- Chen, X., & Shu, L. (2005, December 13). *Stream-Aquifer Interactions: Evaluation of Depletion Volume and Residual Effects from Ground Water Pumping—Chen—2002—Groundwater—Wiley Online Library*. National Groundwater Association.
https://ngwa.onlinelibrary.wiley.com/doi/abs/10.1111/j.1745-6584.2002.tb02656.x?casa_token=S8ukzIjw34gAAAAA:dNPkmn8R5c10Ilg2Ec7tfFiGgcC-KfqdluMS3NfRvgxRYmZF3wMiyobZMYnIL-ZMAvdzRw5umRDfYpmo
- Chen, X., & Yin, Y. (2005, December 13). *Semianalytical Solutions for Stream Depletion in Partially Penetrating Streams—Chen—2004—Groundwater—Wiley Online Library*. National Groundwater Association.
https://ngwa.onlinelibrary.wiley.com/doi/abs/10.1111/j.1745-6584.2004.tb02454.x?casa_token=ywz9jorEOOoAAAAA:DJ6awfB70l1gj0lj8nP6OvLV43rIVGkFUzQ1DqaD200xNSEwrrdP1ITig5-t2-HfzH8Y0xmQ7UjQI-M
- Cherry, J. A. (1990). *Groundwater Monitoring: Some Deficiencies and Opportunities*. Waterloo Centre for Groundwater Research. http://www.gfredlee.com/Groundwater/cherry_gw.pdf
- Christensen, S. (2005, December 13). *On the Estimation of Stream Flow Depletion Parameters by Drawdown Analysis*. <https://ngwa.onlinelibrary.wiley.com/doi/10.1111/j.1745-6584.2000.tb02708.x>
- Condon, L. E., & Maxwell, R. M. (2019). Simulating the sensitivity of evapotranspiration and streamflow to large-scale groundwater depletion. *Science Advances*, 5(6), eaav4574.
<https://doi.org/10.1126/sciadv.aav4574>
- Cooley, J. W., & Tukey, J. W. (1965). An algorithm for the machine calculation of complex Fourier series. *Mathematics of Computation*. <https://www.jstor.org/stable/2003354>
- County of San Luis Obispo Flood Control Map, San Luis Obispo Creek Watershed. 8/19/2019
<https://www.slocounty.ca.gov/Departments/Public-Works/Current-Public-Works-Projects/SLO-Watershed/Watersheds/South-County/San-Luis-Obispo-Creek.aspx>
- Darcy, H. (1856). *The public fountains of the city of Dijon*. Victor Dalmont.
- de Wrachien, D., & Fasso, C. A. (2002). Conjunctive use of surface and groundwater: Overview and perspective. *Irrigation and Drainage*, 51(1), 1–15. <https://doi.org/10.1002/ird.43>

- Dobriyal, P., Badola, R., Tuboi, C., & Hussain, S. A. (2017). A review of methods for monitoring streamflow for sustainable water resource management. *Applied Water Science*, 7(6), 2617–2628. <https://doi.org/10.1007/s13201-016-0488-y>
- Domenico, P. A., & Schwartz, F. W. (1990). *Physical and Chemical Hydrogeology*. Cambridge University Press. <https://www.cambridge.org/core/journals/geological-magazine/article/abs/p-a-domenico-f-w-schwartz-1990-physical-and-chemical-hydrogeology-xxii-824-pp-new-york-chichester-brisbane-toronto-singapore-john-wiley-sons-price-5380-hard-covers-1895-paperback-isbn-0-471-50744-x-0-471-52987-7-pb/2CD74136BA610B7D0D0409F36021100B>
- Foglia, L., Neumann, J., Tolley, D., Orloff, S., Snyder, R., & Harter, T. (2018). Modeling guides groundwater management in a basin with river–aquifer interactions. *California Agriculture*, 72(1), 84–95.
- Freeman, L. A., Carpenter, M. C., Rosenberry, D. O., Rousseau, J. P., Unger, R., & McLean, J. S. (2004). *Use of Submersible Pressure Transducers in Water-Resources Investigations: Vol. Book A, Instrumentation*. United States Geologic Survey.
- Glover, R. E., & Balmer, G. G. (1954). River depletion resulting from pumping a well near a river. *Transactions, American Geophysical Union*, 35, 468–470. <https://doi.org/10.1029/TR035i003p00468>
- Hansen, K. (2017). Chapter 1.1—Meeting the Challenge of Water Scarcity in the Western United States. In J. R. Ziolkowska & J. M. Peterson (Eds.), *Competition for Water Resources* (pp. 2–18). Elsevier. <https://doi.org/10.1016/B978-0-12-803237-4.00001-X>
- Hantush, M. S. (1965). Wells near streams with semipervious beds. *Journal of Geophysical Research (1896-1977)*, 70(12), 2829–2838. <https://doi.org/10.1029/JZ070i012p02829>
- Harbaugh, A. W. (2005). MODFLOW-2005: The U.S. Geological Survey modular ground-water model—the ground-water flow process. In *MODFLOW-2005: The U.S. Geological Survey modular ground-water model—The ground-water flow process* (USGS Numbered Series 6-A16; Techniques and Methods, Vols. 6-A16). <https://doi.org/10.3133/tm6A16>

- Hsieh, P. A., Bredehoeft, J. D., & Rojstaczer, S. A. (1988). Response of well aquifer systems to Earth tides: Problem revisited. *Water Resources Research*, 24(3), 468–472. <https://doi.org/10.1029/WR024i003p00468>
- Huang, C.-S., Wang, Z., Lin, Y.-C., Yeh, H.-D., & Yang, T. (2020). New Analytical Models for Flow Induced by Pumping in a Stream-Aquifer System: A New Robin Boundary Condition Reflecting Joint Effect of Streambed Width and Storage. *Water Resources Research*, 56, e2019WR026352. <https://doi.org/10.1029/2019WR026352>
- Hunt, B. (1999). Unsteady Stream Depletion from Ground Water Pumping. *Groundwater*, 37(1), 98–102. <https://doi.org/10.1111/j.1745-6584.1999.tb00962.x>
- Hunt, B. (2003). Field-Data Analysis for Stream Depletion. *Journal of Hydrologic Engineering*, 8(4), 222–225. [https://doi.org/10.1061/\(ASCE\)1084-0699\(2003\)8:4\(222\)](https://doi.org/10.1061/(ASCE)1084-0699(2003)8:4(222))
- Hunt, B. (2009). Stream Depletion in a Two-Layer Leaky Aquifer System. *Journal of Hydrologic Engineering*, 14(9), 895–903. [https://doi.org/10.1061/\(ASCE\)HE.1943-5584.0000063](https://doi.org/10.1061/(ASCE)HE.1943-5584.0000063)
- Hunt, B. (2014). Review of Stream Depletion Solutions, Behavior, and Calculations. *Journal of Hydrologic Engineering*, 19(1), 167–178. [https://doi.org/10.1061/\(ASCE\)HE.1943-5584.0000768](https://doi.org/10.1061/(ASCE)HE.1943-5584.0000768)
- Hvorslev, M. J. (1951). *Time lag and soil permeability in ground-water observations*. U.S. Army Engineer Waterways Experiment Station. chrome-extension://efaidnbmnnnibpcajpcglclefindmkaj/https://www.csus.edu/indiv/h/hornert/geol_210_summer_2012/week%203%20readings/hvorslev%201951.pdf
- Jaber, F. H., & Shukla, S. (2012, January 1). *MIKE SHE: Model Use, Calibration, and Validation*. <https://doi.org/10.13031/2013.42255>
- Jenkins, C. T. (1968). Techniques for Computing Rate and Volume of Stream Depletion by Wells. *Groundwater*, 6(2), 37–46. <https://doi.org/10.1111/j.1745-6584.1968.tb01641.x>
- Kalbus, E., Reinstorf, F., & Schirmer, M. (2006). Measuring methods for groundwater – surface water interactions: A review. *Hydrology and Earth System Sciences*, 10(6), 873–887. <https://doi.org/10.5194/hess-10-873-2006>

- Kenny, J., Barber, N., Huston, S., Linsey, K., Lovelace, J., & Maupin, M. (2009, October 9). *USGS Circular 1344: Estimated Use of Water in the United States in 2005*.
<https://pubs.usgs.gov/circ/1344/>
- Kollet, S. J., & Zlotnik, V. A. (2003). Stream depletion predictions using pumping test data from a heterogeneous stream–aquifer system (a case study from the Great Plains, USA). *Journal of Hydrology*, 281, 96–114.
- Lackey, G., Neupauer, R. M., & Pitlick, J. (2015). Effects of Streambed Conductance on Stream Depletion. *Water*, 7(1), Article 1. <https://doi.org/10.3390/w7010271>
- Lapides, D. A., Maitland, B. M., Zipper, S. C., Latzka, A. W., Pruitt, A., & Greve, R. (2022). Advancing environmental flows approaches to streamflow depletion management. *Journal of Hydrology*, 607, 127447. <https://doi.org/10.1016/j.jhydrol.2022.127447>
- Leake, S. A., Greer, W., Watt, D., & Weghorst, P. (2008). *Use of Superposition Models to Simulate Possible Depletion of Colorado River Water by Ground-Water Withdrawal*.
<https://pubs.usgs.gov/sir/2008/5189/>
- Li, Q., Gleeson, T., Zipper, S. C., & Kerr, B. (2022). Too Many Streams and Not Enough Time or Money? Analytical Depletion Functions for Streamflow Depletion Estimates. *Ground Water*, 60(1), 145–155. <https://doi.org/10.1111/gwat.13124>
- Lough, H. K., & Hunt, B. (2006). Pumping Test Evaluation of Stream Depletion Parameters. *Groundwater*, 44(4), 540–546. <https://doi.org/10.1111/j.1745-6584.2006.00212.x>
- Lundquist, J. D., & Cayan, D. R. (2002). Seasonal and Spatial Patterns in Diurnal Cycles in Streamflow in the Western United States. *Journal of Hydrometeorology*, 3(5), 591–603.
[https://doi.org/10.1175/1525-7541\(2002\)003<0591:SASPID>2.0.CO;2](https://doi.org/10.1175/1525-7541(2002)003<0591:SASPID>2.0.CO;2)
- MacAllister, D. J., Jackson, M. D., Butler, A. P., & Vinogradov, J. (2016). Tidal influence on self-potential measurements. *Journal of Geophysical Research: Solid Earth*, 121(12), 8432–8452. <https://doi.org/10.1002/2016JB013376>
- Malama, B., Lin, Y.-F., Yu, H.-L., Tseng, H.-T., & Greene, S. (2022). Transient Theory of Pumping Induced Depletion and Drawdown of a Stream with Finite Channel Storage.

Hydrology and Earth System Sciences Discussions, 1–49. <https://doi.org/10.5194/hess-2022-353>

- Malama, B., Pritchard-Peterson, D., Jasbinsek, J. J., & Surfleet, C. (2021). Assessing Stream-Aquifer Connectivity in a Coastal California Watershed. *Water*, 13(4), Article 4. <https://doi.org/10.3390/w13040416>
- Miro, M. E., & Famiglietti, J. S. (2019). A framework for quantifying sustainable yield under California's Sustainable Groundwater Management Act (SGMA). *Sustainable Water Resources Management*, 5(3), 1165–1177. <https://doi.org/10.1007/s40899-018-0283-z>
- Mullen, K. (2022, October 28). *Groundwater | Information on Earth's water*. National Groundwater Association. <https://www.ngwa.org/what-is-groundwater/About-groundwater/information-on-earths-water>
- Neupauer, R. M., Lackey, G., & Pitlick, J. (2020). *Exaggerated Stream Depletion in Streams with Spatiotemporally Varying Streambed Conductance*. *Journal of Hydrologic Engineering*. https://drive.google.com/file/d/1_7uF_9_BP1QWJrm1tSvbEIHtRTVpRR4S/view?usp=embed_facebook
- Rantz, S. E. (1982). *Measurement and Computation of Streamflow: Volume 1 Measurement of Stage and Discharge*. U.S. Geologic Survey.
- Rojstaczer, S., & Riley, F. S. (1990). Response of the water level in a well to Earth tides and atmospheric loading under unconfined conditions. *Water Resources Research*, 26(8), 1803–1817. <https://doi.org/10.1029/WR026i008p01803>
- Rus, D. L., McGuire, V. L., Zurbuchen, B. R., & Zlotnik, V. A. (2001). *Vertical Profiles of Streambed Hydraulic Conductivity Determined Using Slug Tests in Central and Western Nebraska*. *Papers in the Earth and Atmospheric Sciences*.
- Saravanan, S., Parthasarathy, K. S. S., & Sivaranjani, S. (2019). Chapter 10 - Assessing Coastal Aquifer to Seawater Intrusion: Application of the GALDIT Method to the Cuddalore Aquifer, India. In Mu. Ramkumar, R. A. James, D. Menier, & K. Kumaraswamy (Eds.), *Coastal Zone Management* (pp. 233–250). Elsevier. <https://doi.org/10.1016/B978-0-12-814350-6.00010-0>

- State of California. (2014). *Sustainable Groundwater Management Act (SGMA)*.
<https://water.ca.gov/Programs/Groundwater-Management/SGMA-Groundwater-Management>
- Theis, C. V. (1935). The relation between the lowering of the Piezometric surface and the rate and duration of discharge of a well using ground-water storage. *Eos, Transactions American Geophysical Union*, 16(2), 519–524. <https://doi.org/10.1029/TR016i002p00519>
- Theis, C. V. (1941). The effect of a well on the flow of a nearby stream. *Eos, Transactions American Geophysical Union*, 22(3), 734–738. <https://doi.org/10.1029/TR022i003p00734>
- Thomas, B. F. (2019). Sustainability indices to evaluate groundwater adaptive management: A case study in California (USA) for the Sustainable Groundwater Management Act. *Hydrogeology Journal*, 27(1), 239–248. <https://doi.org/10.1007/s10040-018-1863-6>
- Turnipseed, D. P., & Sauer, V. B. (2010). *Discharge Measurements at Gaging Stations*. United States Geologic Survey.
- USGS, U. S. G. S. (2023, June 27). *Groundwater Modeling | USGS California Water Science Center*. <https://ca.water.usgs.gov/projects/central-valley/groundwater-modeling.html>
- Wang, W., Dai, Z., Zhao, Y., Li, J., Duan, L., Wang, Z., & Zhu, L. (2016). A quantitative analysis of hydraulic interaction processes in stream-aquifer systems. *Scientific Reports*, 6(1), Article 1. <https://doi.org/10.1038/srep19876>
- Ward, N. D., & Callander, P. (2010). Distribution of Stream Depletion. *Journal of Hydraulic Engineering*, 136(3), 170–174. [https://doi.org/10.1061/\(ASCE\)HY.1943-7900.0000137](https://doi.org/10.1061/(ASCE)HY.1943-7900.0000137)
- WEF. (2020, June 22). *Groundwater Banking*. Water Education Foundation.
<https://www.watereducation.org/aquapedia/groundwater-banking>
- West | U.S. Drought Monitor. (2023, June 27).
<https://droughtmonitor.unl.edu/CurrentMap/StateDroughtMonitor.aspx?West>
- Winter, T. C., Harvey, J. W., Franke, O. L., & Alley, W. M. (1998). Ground water and surface water: A single resource. In *Ground water and surface water: A single resource* (USGS Numbered Series 1139; Circular, Vol. 1139). U.S. Geological Survey.
<https://doi.org/10.3133/cir1139>

- Zipper, S. C., Farmer, W. H., Brookfield, A., Ajami, H., Reeves, H. W., Wardropper, C., Hammond, J. C., Gleeson, T., & Deines, J. M. (2022). Quantifying Streamflow Depletion from Groundwater Pumping: A Practical Review of Past and Emerging Approaches for Water Management. *Journal of the American Water Resources Association*, 58, 289–312. <https://doi.org/10.1111/1752-1688.12998>
- Zlotnik, V., Huang, H., & Butler, J. (1999). Evaluation of Stream Depletion Considering Finite Stream Width, Shallow Penetration, and Properties of Streambed Sediments. *Papers in the Earth and Atmospheric Sciences*.
<https://digitalcommons.unl.edu/geosciencefacpub/145>